universität wien

DIPLOMARBEIT

Titel der Diplomarbeit

Verification of Dscam expression in rat microglia

angestrebter akademischer Grad

Magister der Naturwissenschaften (Mag. rer.nat.)

Verfasser:	Roland Prielhofer
Matrikel-Nummer:	0400857
Studienrichtung:	A490 - Molekulare Biologie
Betreuerin	Univ.-Doz. Dr. Monika Bradl (Medizinische Universität Wien)

Wien, August 2009

Table of contents:

Abstract

Microglia cells are specialized macrophages, found throughout the brain and spinal cord. Two functional distinct populations have been characterized on the basis of the expression of an antibody (5D4) reactive keratan sulfate proteoglycan on their cell surface. Cells with lower expression ($5D4^{low}$) are more immunologically active than their highly expressing ($5D4^{high}$) counterparts. $5D4^{high}/5D4^{low}$- comparative microarray data revealed many differentially expressed genes which were of particular interest with respect to microglia development and function. Five genes, which showed an increased expression rate in $5D4^{high}$ microglia cells, were analyzed: Cadm1, Dlx2, Dscam, Tef and Twist-2. All of them, besides Cadm1, were found to be active on the mRNA level in rat microglia cells.

The role of Dscam in the immune system of Drosophila and its ability to make homo- and heterophilic interactions was very interesting in this aspect. Hence, it was the most promising aspirant for further investigations. We focused on Dscam and examined its expression on mRNA and protein level in rat microglia cells. Additionally, a functional knock-down experiment was performed.

Even though Dscam expression was shown several times, we could not clearly confirm its expression in rat microglia cells, since the presence of false positive cells, possible due to Dscam positive contaminants could not be completely excluded.

Future studies should be done to further address the possible role of Dscam in mammalian immune responses. Helpful in this regard would be more and novel literature about microglia diversity as well as the development of an appropriate antibody.

Zusammenfassung

Mikrogliazellen sind spezialisierte Makrophagen, die im Gehirn und Rückenmark vorkommen. Basierend auf der Expression eines Antikörper (5D4)- reaktiven Keratansufat-Proteoglykans auf der Oberfläche der Zellen konnten zwei funktionell unterschiedliche Populationen charakterisiert werden. Zellen mit geringerer Expression ($5D4^{low}$) sind immunologisch aktiver, als jene mit hoher Expression ($5D4^{high}$). Ein Vergleich von $5D4^{high}$- und $5D4^{low}$- Microarray Daten führte zur Entdeckung vieler Gene, welche im Bezug auf Entwicklung und Funktion von Mikrogliazellen von großem Interesse sein könnten. Fünf Gene, welche eine erhöhte Expressionsrate in $5D4^{high}$ Mikrogliazellen zeigten, wurden untersucht: Cadm1, Dlx2, Dscam, Tef und Twist-2. Die Expression aller Gene außer Cadm1 konnte auf mRNA Ebene nachgewiesen werden.

Für unsere Fragestellung war Dscam aufgrund seiner Funktion im Immunsystem von Drosophila und wegen seiner homo- und heterophiler Interaktionen sehr interessant. Deshalb entschieden wir uns, die Expression von Dscam in Mikrogliazellen auf mRNA- und Protein-Ebene genauer zu untersuchen. Zusätzlich führten wir ein funktionelles Knock-Down Experiment durch.

Obwohl wir Dscam mehrmals nachweisen konnten, war es uns nicht möglich seine Expression in Ratten- Mikrogliazellen definitiv zu bestätigen, da mögliche falsch positive Zellen nicht mit Sicherheit ausgeschlossen werden konnten.

Zukünftige Studien sollten die Rolle von Dscam im Säugetier- Immunsystem verifizieren. Weitere Erkenntnisse über Mikroglia- Diversität und die Entwicklung eines neuen, geeigneten Antikörpers könnten dabei zielführend sein.

Introduction

Approximately 20% of the total glial cell population in the central nervous system comprise of microglial cells (MG), which belong to the mononuclear phagocyte system and form the resident macrophages in the brain tissue, the spinal cord and the retina (Kreutzberg, 1995).

MG populate the CNS first during early development, deriving from progenitors whose origin is the yolk sac (Figure 1, Alliot et al., 1999) and second via the supraventricular corpus callosum consisting of cells originating from bone marrow-derived myeloid progenitor cells (Ritter et al., 2006), named as "Fountain of microglia" (Del Rio-Hortega, 1932).

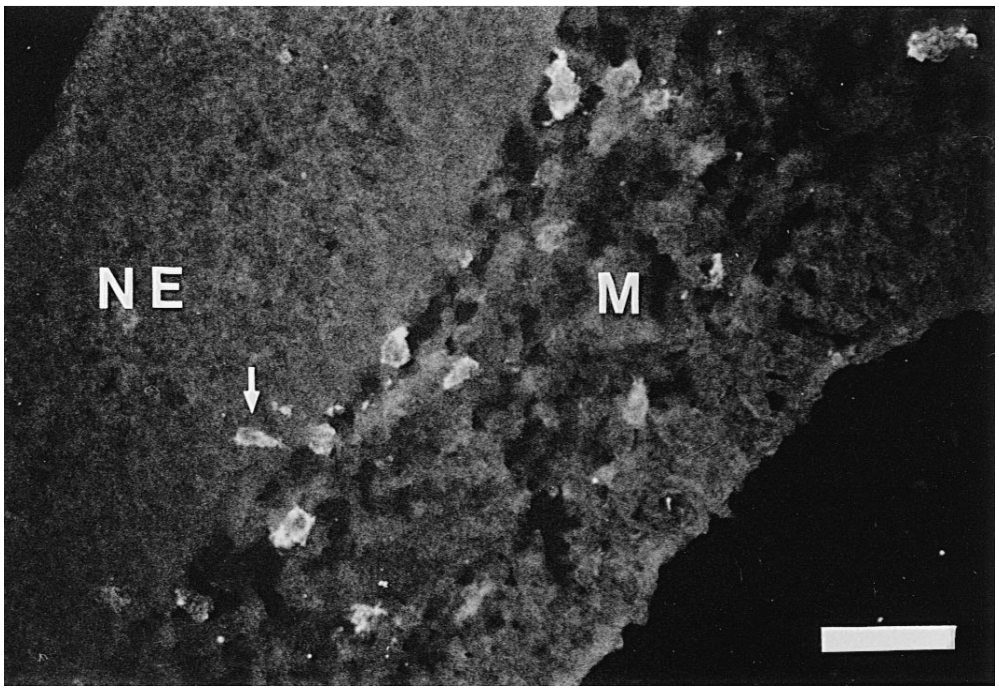

Figure 1. Cross section through a mouse brain rudiment (E10). Bright cells are F4/80 positive (macrophage/microglial marker), and thereby represent cells of the mononuclear phagocyte system, which are initially found in the mesenchyme (M). Some of them (see arrow) infiltrate the neuroepithelium (NE) and eventually become microglia. Bar equals 40 μm (Figure taken from Alliot et al., 1999).

These cells actively proliferate locally and disperse throughout brain and spinal cord tissue (Alliot et. al, 1999).

MG assume an important local surveillance role, they remove dead cells and other debris from their surroundings and they express receptors for complement, immunoglobulin and apoptotic-cell surface markers. In the normal brain, these resting microglia are highly

ramified (Raivich, 2005). Activating stimuli lead to secretion of a large number of different factors, with which they play a role in tissue destruction and tissue repair/protection. Hence, they were termed "sensors of CNS pathology". Profound knowledge of intercellular signalling pathways of proliferation/activation in microglia could be a basis for targeted intervention on glial reactions in the CNS (Kreutzberg, 1996).

Recent studies showed that there are two different microglia populations in the rat, based on the expression of an antibody-reactive keratan sulfate proteoglycan (KSPG) on their cell surface. This antibody, named "5D4", reacts with 50 % of all ramified MG. These $5D4^{high}$ MG are nicely intermingled with $5D4^{low}$ cells throughout the brain tissue (Figure 2, Jones and Tuszynski, 2002).

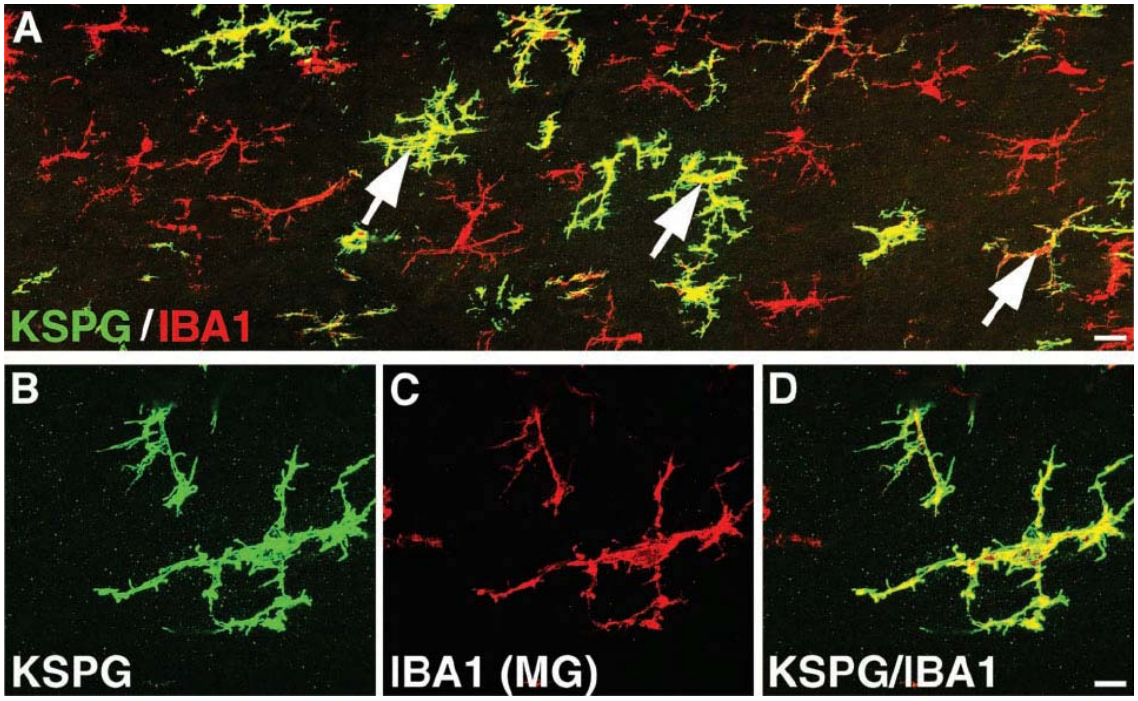

Figure 2. KSPG expression by MG in the intact spinal cord. The 5D4 reactive KSPG is expressed throughout the intact spinal cord on a subpopulation of MG but not on oligodendrocyte progenitors and astrocytes. *A*, Composite of three confocal images taken from the dorsal white matter. 5D4 reactive KSPG, *green*; MG/macrophage marker IBA1, *red*. *Arrows* indicate examples of ramified MG expressing 5D4-KSPG. Scale bar, 135 µm. *B–D*, High magnification of 5D4 reactive KSPG and IBA1 MG. 5D4 reactive KSPG immunoreactivity encompasses the soma and cell processes. Scale bar, 5 µm (Figure and legend taken from Jones and Tuszynski, 2002)

There are two facts, supporting the assumption that these two populations vary in their functionality:

First, two different microglia populations had also been discovered in the adult murine CNS, based on the expression of the innate microglial immune receptor TREM-2 (triggering

receptor expressed on myeloid cells-2). Both populations, TREM-2 positive and negative, exist side by side and differ in their functions, regarding phagocytosis or mediation of proinflammatory responses (Schmid et al., 2002; Takahashi et al., 2005).

Second, this hypothesis is also supported by current knowledge of 5D4 reactive KSPG:: Keratan sufate proteoglycan expression on the cell surface remains stable in Wallerian degeneration of axotomized fiber tracts (Jander and Stoll, 1996); KSPG expression is increased under ischaemic conditions (Zhang et al., 2005) as well as subsequent to spinal cord injury (Jones and Tuszynski, 2002); and it disappears from the surface of $5D4^{high}$ microglia cells due to experimental autoimmune encephalomyelitis (EAE), an inflammatory demyelinating disease of the CNS (Jander et al., 2000).

Microarray studies on $5D4^{high}$ and $5D4^{low}$ microglia cells showed that these populations clearly differ in their expression profile and in their response to pathological conditions:

$5D4^{low}$ MG seem to be immunological more active than their $5D4^{high}$ counterparts, because they express more genes belonging to the following categories: innate defense molecules, receptors, factors involved in LPS response, "cytokines, chemokines and other attractants", "proteins needed for vesicle traffic, exocytosis and phagocytosis", intracellular signalling molecules, proteins of the complement cascade and proteins involved in coagulation (Leitner and Bradl, unpublished observation).

Indicating a higher expression rate in $5D4^{high}$ MG than in their $5D4^{low}$ counterpart (Table 1), these following 5 molecules were especially interesting for us: *Cadm1, Dlx2, Dscam, Tef, Twist-2;*

Full Name	**Symbol**	**Target Id**	**p-Value**	**log2Fold Change**
Rattus norvegicus cell adhesion molecule 1	**Cadm1**	NM_001012201	0,00046	1,032
Rattus norvegicus distal-less homeobox 2	**Dlx2**	XM_230986	0,04063	1,109
Rattus norvegicus Down syndrome cell adhesion molecule	**Dscam**	NM_133587	0,00208	1,093
Rattus norvegicus thyrotrophic embryonic factor	**Tef**	NM_019194	0,02887	1,034
Rattus norvegicus twist homolog 2 (Drosophila)	**Twist2**	NM_021691	0,00802	1,512

Table 1. Microarray data of target molecules; p-values and log2fold expression in $5D4^{high}$ relative to $5D4^{low}$ microglia;

All these molecules might play an important role in microglia development and function:

- Cell adhesion molecule 1 (Cadm1, Necl-2) is an adhesion molecule, primarily expressed on cytotoxic T cells, involved in tumor suppression, synapse formation, and spermatogenesis. It defines a specialized subset of DCs in both mouse and

human. Cadm1 a ligand for class I MHC-restricted T-cell associated molecule (Crtam) and it was proposed that this molecular pair could regulate a large panel of cell/cell interactions both within and outside of the immune system (Galibert et al., 2005).

- Dlx2: A homeobox transcription factor family, called Distall-less (Dlx), primarily implicated in murine development, had been analyzed in natural killer cells (NK). Therefore a gene expression profile approach was performed, using a mouse model in which NK cells are arrested at an immature stage of development. It could be demonstrated, that Dlx1, Dlx2, and Dlx3 are transiently expressed in immature Mac-1^{lo} NK cells. These genes are expressed in a temporally regulated pattern with overlapping waves of expression, and they display functional redundancy. It was observed that persistent expression of Dlx genes leads to functionally immature NK cells arrested at the Mac-1^{lo} stage and that T and B cells fail to develop in the context of continuing Dlx1 expression. Thus, these studies indicate that Dlx transcription factors play a functional role in lymphocyte development (Sunwoo et al., 2008).
- *Down syndrome cell adhesion molecule (Dscam)* was first described in neuronal development. Recent studies present Dscam in a new context: D. melanogaster immune tissues can express more than 18,000 different extracellular domains of Dscam and soluble forms of Dscam have also been identified in cell supernatants and in the haemolymph. Dscam potentially acts as both a phagocytic receptor and an opsonin. This suggestion is supported by the identification of Dscam in the phagosome proteome of Drosophila. The crystal structures of two Dscam isoforms reveal each one with two distinct surface epitopes, one on either side of the receptor. This configuration allows a given Dscam isoform to form a homodimer (epitope I) and retain the ability to recognize, opsonize and crosslink pathogens (epitope II) (Stuart and Ezekowitz, 2008). A horseshoe-shaped configuration was observed by crystallographic analyses of D1-$D4_{1.34}$ (splice variant 1 of exon 4 and splice variant 34 of exon 6) proteins of Dscam (Figure 3, Meijers et al., 2007).

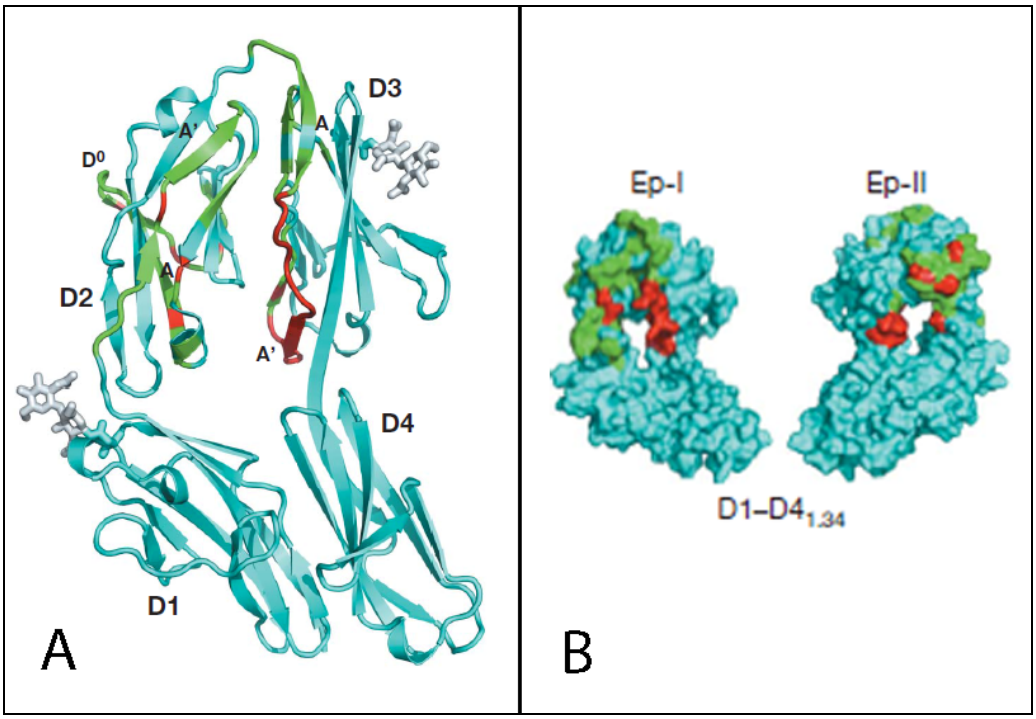

Figure 3. Horseshoe- shaped structure of Dscam D1-D4$_{1.34}$: Ribbon diagram (A) and surface representation of epitope I (left) and II (right) on either side of molecule (B). Colour code: conserved residues are coloured cyan, variable residues are green and hypervariable residues are red (Figure taken from Meijers et al., 2007).

A limited set of homophilic binding interfaces implicate a high evolutionary selection pressure, and thereby a strong sequence conservation in epitope I. Whereas epitope II was shown to be a faster evolving sequence, consistent with immune receptor adaptations to dynamic alterations in host– pathogen interactions. Therefore it was hypothesized that this structural separation of homophilic and heterophilic binding (that is potentially self and non-self recognition) in Dscam may have enabled the parsimonious use of the same gene in creating a large receptor diversity in both the nervous system and immune system (Meijers et al., 2007).

- *Tyrotroph embryonic factor (Tef):* Chimeric transcription factors are generated in leukemia, resulting in gain or loss of function of a gene. HLF (E2A- hepatic leukemia factor) contributes to leukemogenesis through its potential to inhibit apoptosis. Physiologic counterparts are of particular interest: Tef was found to share high levels of sequence identity with HLF and recognizes the same DNA sequence. Tef protected IL-3 dependent cells from apoptosis by IL-3 deprivation, due to almost complete down-regulation of the common βc chain of cytokine receptors. These findings suggested that Tef is one of the apoptotic regulators in

hematopoetic progenitors and to control hematopoetic cell proliferation by regulating the expression of cytokine receptor βc chain (Inukai et al., 2005).

- *Twist-2:* Basic helix loop helix transcription factor Twist-2 is described to be a key negative regulator of myeloid linage development. Twist-2 deficient mice showed a marked increase of mature myeloid populations. Interaction with the transcription factors Runx1 and C/EBPα results in their inactivation followed by inhibition of proliferation and differentiation of granulocyte macrophage progenitors. The production of proinflammatory cytokines (IL-12, IFN-γ) is inhibited, while regular cytokines (IL-10) are promoted. In summary, Twist-2 was characterized as a critical factor in regulation of myeloid lineages, as well as in function and inflammatory responses of mature myeloid cells (Sharabi et al., 2008).

Are all of these five molecules really expressed in MG? In an attempt to confirm the microarray data described above, several MG populations were analyzed by PCR to address this point.

Then, we concentrated on Dscam, since its action as phagocytic receptor and as an opsonin in Drosophila was particularly interesting to us with respect to macrophage/microglia cell function.

1. Material and Methods

1.1. Cell biology

1.1.1. Media

Microglia culture medium

RPMI 1640 without L-Glutamine (Lonza Group, Ltd. Basel, Switzerland) was supplemented by 10 % (v/v) Fetal Bovine Serum (FBS; Lonza Biowhittaker®), 1 % (v/v) Penicillin/Streptavidin (10.000 U/ml, Lonza Biowhittaker®) and 1 % (v/v) L- Glutamin (200 mM in 0,85 % NaCl) – (Lonza Biowhittaker®). Glutamine is an unstable essential amino acid and is therefore added prior to use. Microglia culture medium was prepared fresh and used for four to five days at most.

RPMI 1640, **R**oswell **P**ark **M**emorial **I**nstitute medium, is a typical medium used in cell cultures and contains glucose, salts, amino acids and vitamins. It is intended to be used in a 5 % carbon dioxide atmosphere because of its contained phosphate-buffer system.

Microglia medium with reduced FBS concentration, 5 % (v/v), was used for knockdown experiments with Endo-Porter and Morpholios.

FBS is derived from blood drawn from bovine fretuses. It's the most widely used serum and is used for growing eukaryotic cells. Bovine serum albumin, BSA, the globular protein, is a major component of FBS.

DMEM (Lonza Biowhittaker®)

Dulbecco´s **M**odified **E**agle **M**edium is a standardized cell culture medium for animal cells. It contains certain amounts of glucose, anorganic salts, amino acids, vitamins and other substances.

Freezing medium

RPMI 1640 without L-Glutamine (Lonza Group, Ltd. Basel, Switzerland) was supplemented with 45 % (v/v) Fetal Bovine Serum (FBS; Lonza Biowhittaker®) and 10 % (v/v) DMSO (≥99 %, Sigma-Aldrich®).

DMSO, **D**i**m**ethyl**s**ulf**o**xyde, is an organic solvent which is used as cryoprotective additive. It prevents the formation of ice crystals which would damage the cells.

1.1.2. Model organisms

Procedures involving animals were performed in consideration of the institutional guidelines. The animals had free access to food and water.

Newborn Lewis rats or newborn C57BL/6N mice were used for microglia cultures. For microglia isolation and purification experiments, 2 to 7 month old Lewis rats were used.

1.1.3. Preparation of primary mixed glial cell cultures

Poly L- lysine (Sigma-Aldrich®, Cat. Nr. P2636) coated cell culture flasks (Greiner Bio One) were washed with sterile PBS and used for culturing of the cells at 37 °C and 5 % CO_2.

Newborn Lewis rats or new born mice were quickly decapitated and the head was kept in a petri dish containing 70 % ethanol. Then the brain was excised, placed in a petri dish containing DMEM and the meninges were removed using two forceps. The brain was then transferred into a petri dish containing microglia medium, homogenized by pipetting and transfered into a washed Poly L- lysine coated cell culture bottle. The formation of a solid mixed glial cell monolayer for microglia production was optimal with one brain in 10 to 15 ml microglia medium per cell culture flask.

After 24 hours the supernatant was aspirated and 10 ml fresh microglia medium was added. After six to seven days of incubation at 37 °C, a cell monolayer developed and microglia cells could be harvested by shaking the flask (rotary shaker, Infors® HT – CH-4103, at 160 to 180 RPM) for one to four hours. Usually a total of three shake offs were performed with a period of three to four days between them so that microglia cells could proliferate again.

1.1.4. BD PuraMatrix™ peptide hydrogel

The PuraMatrix™ hydrogel peptide (Becton Dickinson) is new synthetic material which forms a defined three dimensional microenvironment for a variety of cell-based assays. It consists of standard amino acids (1 % w/v) and 99 % water. The manufactorer´s instruction for "3D Cell Encapsulation in Cell Culture Plates" was used.

First, the BD PuraMatrix stock solution (1 %, w/v) was sonicated in a bath sonicator for 30 min to decrease viscosity. Then one part each, sterile 20 % fructose solution and BD PuraMatrix stock solution, and two parts of $5 \cdot 10^5$ to $10 \cdot 10^5$ microglia cells in sterile 10 % fructose solution were mixed. Fructose was diluted in sterile water, as salts would start the gelation of the gel immediately. The microglia cells were either taken from shake off, frozen or from cold- shock detached plates. Culture media was removed, and the cells were washed and resuspended in sterile 10 % fructose solution.

The mixture was carefully placed in the centre of a well (24-well plate), without introducing any air bubbles. Gelation of the BD PuraMatrix was induced by gently running culture media (RT) down the side of the well on top of the hydrogel. Then the media was changed two times over the next 30 to 60 minutes. 250 µl of the mixture was used per well and 300 µl microglia medium were added.

The setup for Ultramicroscopy (see 1.1.8) was done using 6- well plates, coverslips and small plastic rings (see Figure 4) to obtain cake-shaped BD PuraMatrix pieces. About 1 ml of the mixture and 6 to 8 ml of microglia medium were needed. The plastic ring was carefully removed immediately before investigation, as the gel is easily damageable.

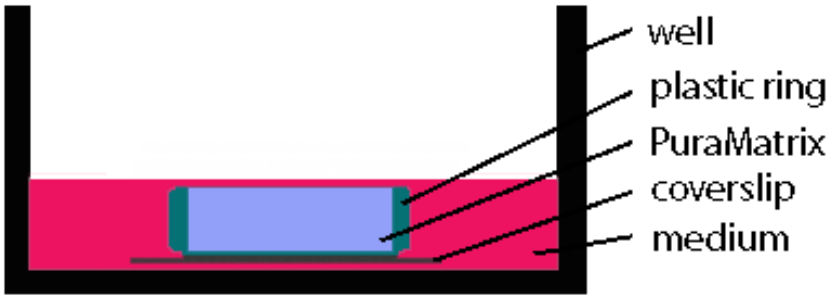

Figure 4. BD PuraMatrix plastic ring Ultramicroscopy setup.

1.1.5. Isolation of microglia from adult lewis rat spinal cords

The animals were killed by CO_2 suffocation. Cardiac arrest was reached within few minutes. The vena cava inferior and the vena portae in the liver were transected and the blood was flushed out of the vasculature by transcardial perfusion with PBS. The spinal cord was taken out, transferred into ice-cold RPMI 1640, and the meninges and processes of the peripheral nerves were removed. Then, the spinal cords were mechanically dissociated through a stainless-steel sieve (screens for CD-1, size 100 mesh, Sigma-Aldrich®). This procedure results in a dissociated single cell suspension. It was collected in 25 ml of RPMI medium (density, $\rho = 1{,}012$ g/ml) in a 50 ml tube (maximal cells from three spinal cords per tube). To this cells suspension, 10,8 ml Percoll™ ($\rho = 1{,}130$ g/ml at RT) (Amersham Biosciences) were added. The final cell suspension then had a density of $\rho = 1{,}048$ g/ml.

For the density gradient centrifugation 400 µl of distilled water and 10 ml Percoll™ were mixed to $\rho = 1{,}125$ g/ml and carefully added to the cell suspension. Since this Percoll™ solution had a higher density than the cell suspension, the newly added Percoll/H_2O solution formed a cushion underneath the cell suspension.

This gradient was centrifuged at 3.000·g for 40 min at RT (no brake to avoid mixing of the different phases). The myelin debris on top of the solution was aspirated and the microglia cells and macrophages were collected from the clear phase of the upper layer (see Figure 5).

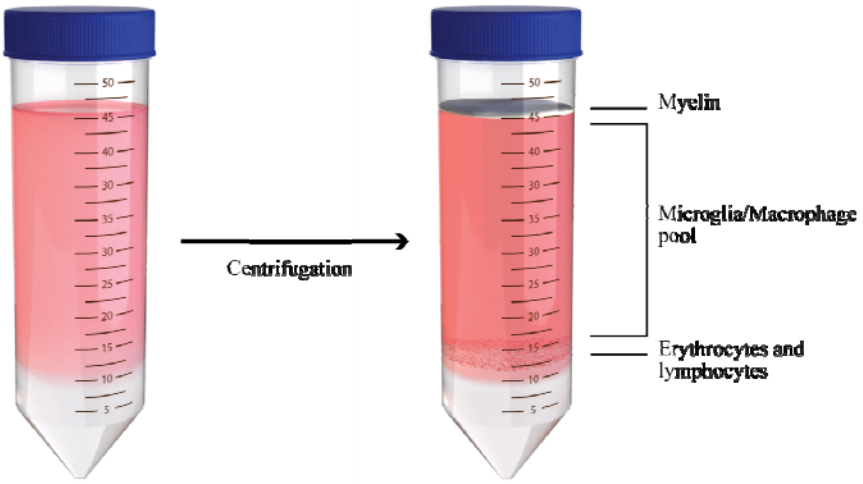

Figure 5. Desity gradient centrifugation, phase profile before and after centrifugation (figure kindly provided by Rui Martins).

The cells were harvested in approximately 25 ml medium into a new 50 ml centrifuge tube and were pelleted by centrifugation at 1.400·g for 30 min at RT. Then, all supernatant was removed except of 200 µl. The cell pellet was resuspended in the remaining supernatant and centrifuged again at 1.400·g for 10 min at RT. Finally, the supernatant was removed and the pellet was resuspended in 200 µl medium.

1.1.6. Lymphocyte isolation

The blood was collected in a tube containing anticoagulant and diluted by adding an equal volume of 0,9 % NaCl. Then 6 ml of the diluted blood were layered on top of 3 ml of Lymphoprep™. This was followed by centrifugation at 800·g for 20 minutes. Mononuclear cells were taken from the distinct band at the sample/media interface (see Figure 5).

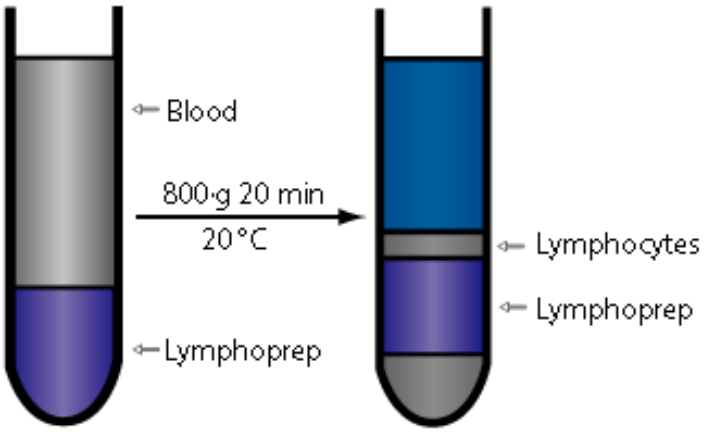

Figure 6. Lymphoprep™, AXIS-SHIELD (Figure adapted from http://search.cosmobio.co.jp/).

1.1.7. Phase-contrast microscopy and imaging

An inverted microscope (DM IL, Leica® Microsystems) attached to an SLR CCD Camera (E-300, Olympus) was used for microscopy of the cells in the petri dishes and flasks through 10X, 20X, and 40X objective lenses and phase-contrast optics.

1.1.8. Ultramicroscopy

This method was developed to visualize individual cells and cellular structures in opaque objects (Dodt et al., 2007). The basic principle of this method (Figure 7) is the immersion of the specimen in a medium with the same refractive index as protein. This allows 3D imaging with micrometer resolution of macroscopic samples.

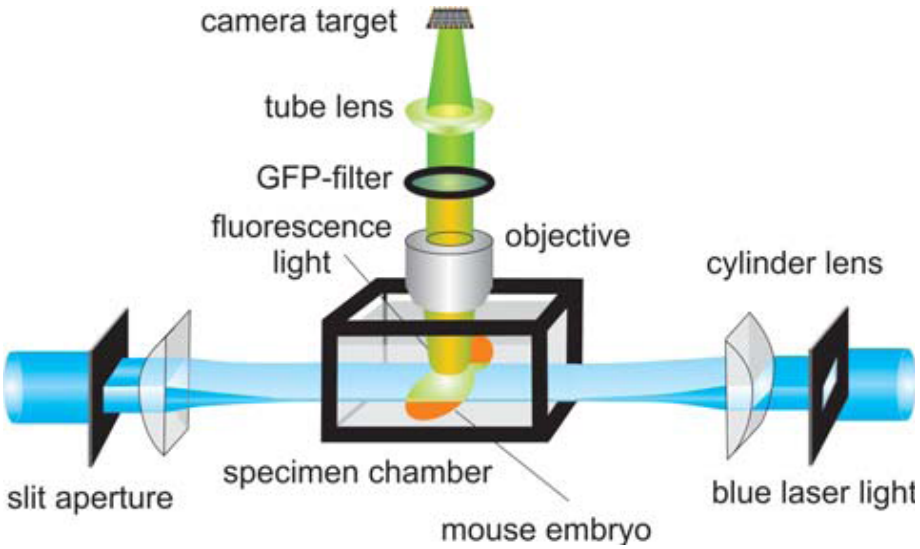

Figure 7. Principle of ultramicroscopy. The sample is illuminated by a blue laser forming a thin sheet of light. Fluorescent light is thus emitted only from a thin optical section and collected by the objective lens. (Figure taken from Dodt et al., 2007).

The cells in the PuraMatrix peptide hydrogel were stained with tomato-lectin- FITC conjugate (see 1.3.1) which was added to the medium. After incubation for 30 minutes the gel was rinsed and washed with fresh medium very carefully. Lectins are very specific sugar-binding proteins and are often used by viruses to attach themselves to their host cells.

1.2. Molecular Biology

1.2.1. Isolation of total RNA, DNAse digestion and RNA Cleanup

The Quiagen RNeasy® Mini Kit was used to isolate total RNA according to the manufacturer's instructions. This was followed by elimination of genomic DNA contamination by DNAase digestion. 7 µl 10X DNase I Buffer (Fermentas), 7 µl DNase I (1 u/µl, Fermentas) and 2 µl Ribolock® RNase inhibitor (40 u/µl, Fermentas) were added to

54 µl of total RNA sample and incubated at 37ºC for 30 minutes. Then 7 µl EDTA were added and the sample was incubated at 65 ºC for 10 min to chelate and stop the reaction.

Total RNA was then further purified using the Quiagen RNeasy® Mini Kit according to the RNA Cleanup- protocol.

1.2.2. Reverse Transcription

Starting from total RNA after RNA Cleanup, cDNA was obtained by reverse transcription. First, 2 µl of random primers (T7-N7) were added to each sample and incubated at 70 °C for 5 min and another 5 min on ice. Then 20 µl master mix was added per sample, consisting of the following components:

10 µl	M-MLV 5X RT Buffer (Promega Corporation)
2,5 µl	PCR grade dNTPs (Roche Applied Science)
2,5 µl	Ribolock® RNase inhibitor (40 u/µl, Fermentas)
5,0 µl	ddH_2O

The sample was incubated at 40 ºC for 2 min, 2 µl M-MLV Reverse Transcriptase (200 u/µl, Promega Corporation) were added, left at RT for 10 minutes and then placed in a thermoblock at 40 ºC for 50 minutes. Finally, the sample was incubated at 70 °C for 15 min. cDNA samples were stored at -20 °C.

1.2.3. Synthesis of DIG- labeled cRNA

DIG RNA Labeling Kit (SP6/SP7) (Roche, Cat.No. 11175025910) was used to produce DIG-labeled cRNA from PCR-products for Northern blot. Labeling quality was analyzed by dot blotting.

The probe must be complementary to the target mRNA. The PCR-product, provided by the T7-tagged forward primer, enables the T7-polymerase to produce mRNA-complementary copy-RNA from mRNA-homolog cDNA (Figure 8). See 1.2.5 for primer sequences.

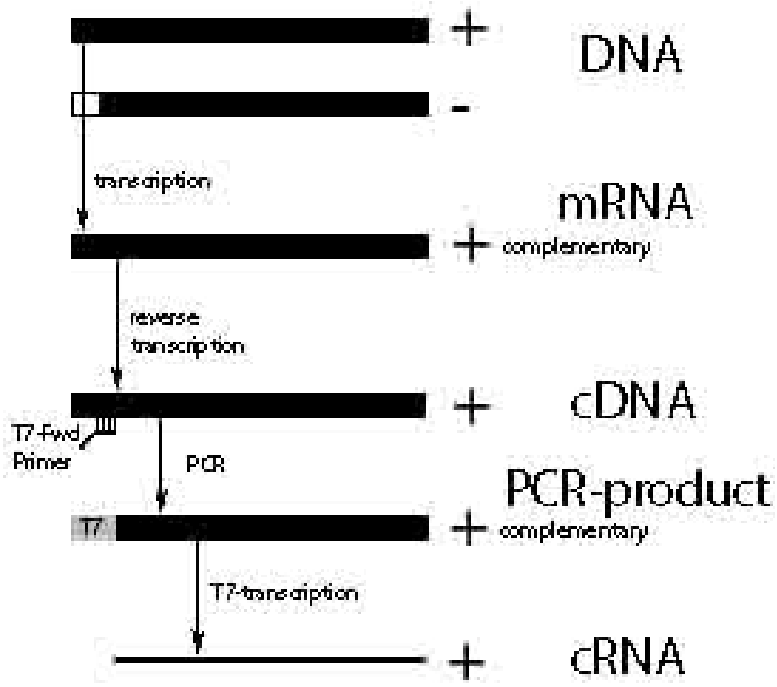

Figure 8. Northern probe preparation

The T7-GAPDH_large- fragment (758 bp) was obtained by PCR from microglia cDNA (Figure 9).

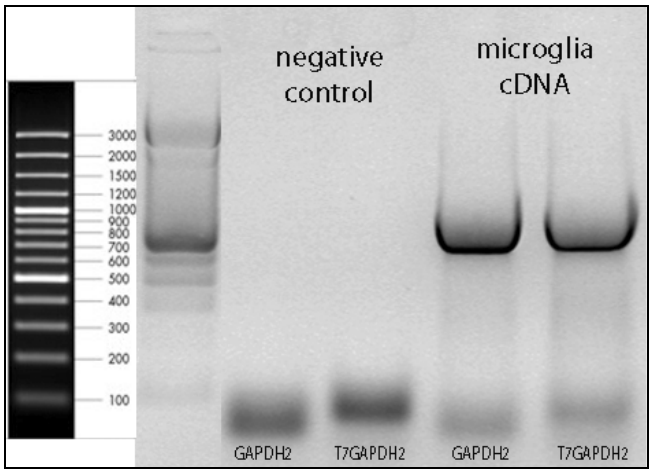

Figure 9. GAPDH_large- probe; negative controls without template; GAPDH_large and T7GAPDH_large PCR products (738 and 758 bp respectively);

The first trial to synthesize the probe for Dscam was not effective to obtain the T7 conjugated Dscam- fragment. So I produced high amounts of the T7- exclusive fragment (Figure 10).

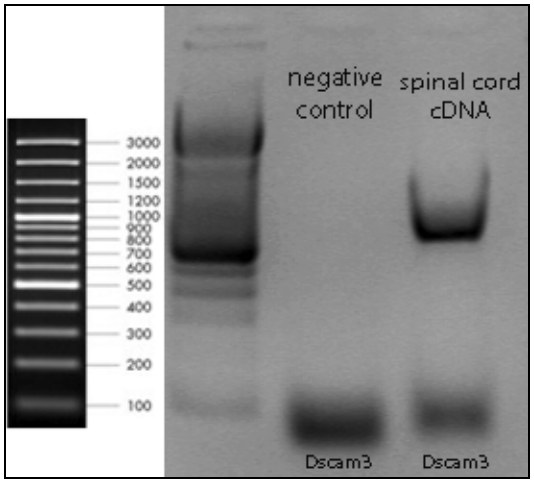

Figure 10. Dscam_large- PCR product (821 bp).

Concentrating in a small volume and using this PCR fragment as template for PCR with the T7- conjugated primer was effective (Figure 11).

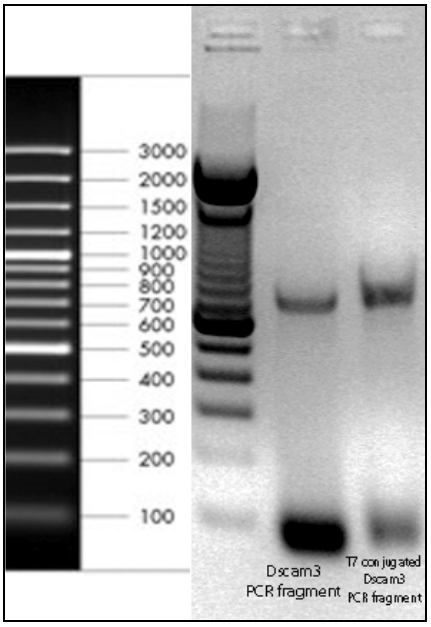

Figure 11. T7-conjugated Dscam_large PCR fragment (841 bp), compared to Dscam_large PCR product (821 bp);

The T7 conjugated PCR products were purified from gel and used for probe preparation.

1.2.4. Dot blot

One µl of 1:5, 1:25 and 1:125 diluted pobe was dropped on a nylon membrane and crosslinked by Stratalinker® UV Crosslinker (Model 1800, #400072). Then it was blocked in Roche Blocking Reagent (Cat.No. 11096176001), supplemented with 10% Fetal Bovine Serum (FBS; Lonza Biowhittaker) over night.

Detection was done using NBT/BCIP (Roche Applied Science) according to the manufacturer's instructions.

1.2.5. PCR and Gelelectrophoresis

For the polymerase chain reaction (PCR), the master mix was prepared fresh from 5 µl PCR Reaction Buffer(10X, 20 mM $MgCl_2$), 1 µl dNTP Mix, 0,4 µl FastStart Taq DNA-Polymerase (5 U/µl) and 1 µl forward and reverse primer for 1 µl template DNA. PCR Reaction buffer, dNTP Mix and Fast Start Taq provided by Roche Applied Bioscience; Biometra® TPersonal thermocycler was used.

Primers were design using the Primer3Plus service (Rozen and Skaletsky, 2000) on the WWW (http://www.genome.wi.mit.edu/cgi-bin/primer/primer3-_www.cgi) provided by Whitehead Institute/MIT Center for Genome Research and ordered from Eurofins MWG GmbH.

Table 2. Primer-sequences and melting temperatures.

Name	Sequence (5´ → 3´)	T_M [°C]	Accession number
Cadm1_Fwd	AGATTCTCGAGCAGGTGAAGAG	60,3	NM_001012201.1
Cadm1_Rev	ATGATGAGCAAACATAGCATGG	56,5	NM_001012201.1
Dlx2_Fwd	TGGAGTCTTTGACAGTCTGGTG	60,3	XM_230986.4
Dlx2_Rev	GTTGGTGTAGTAGCTGCTGTCG	62,1	XM_230986.4
Tef_Fwd	TTGCAGTAGATATGCACCCAAC	58,4	NM_019194.2
Tef_Rev	CTGAGAAGGGATACTGGGTGAC	62,1	NM_019194.2
Twist2_Fwd	AGCAAGAAATCGAGCGAAGAT	55,9	NM_021691.1
Twist2_Rev	CAGCTGGTCATCTTATTGTCCA	58,4	NM_021691.1
ratGAPDH_Fwd	GGCATTGCTCTCAATGACACC	59,8	NM_017008

ratGAPDH_Rev	TGAGGGTGCAGCGAACTTTAT	57,9	NM_017008
ratGAPDH_large_Fwd	GAGTCTACTGGCGTCTTCAC	59,4	NM_017008
ratGAPDH2_large_Rev	GTCCAGGGTTTCTTACTCCT	57,3	NM_017008
T7ratGAPDH_large_Fwd	TAATACGACTCACTATAGGG-GAGTCTACTGGCGTCTTCAC	59,4	NM_017008
Dscam_small_Fwd	CGGACGCATAAGTGAAATCATA	56,5	NM_133587.1
Dscam_small_Rev	GCATCTGCAGTTCATACCATGT	58,4	NM_133587.1
Dscam_middle_Fwd	UCCAAUCACCUCAUUCACUC	55,3	NM_133587.1
Dscam_middle_Rev	TCTCCATTGTGTCTCTCTCT	55,3	NM_133587.1
Dscam_large_Fwd	CACTCCAGCCTCTACTTTGTCAAT	61,0	NM_133587.1
Dscam_large_Rev	GTTATCTTTCAGCCAGCGGTAGTC	62,7	NM_133587.1
T7Dscam_large_Fwd	TAATACGACTCACTATAGGG-CACTCCAGCCTCTACTTTGTCAAT	61,0	NM_133587.1

Gelelectrophoresis was performed in PerfectBlue™ gelelectrophoresis system (PEQLAB Biotechnologie GmbH) with 1 % agarose gel, using 12 µl Ethidium bromide solution (Sigma-Aldrich®) per 300 ml of gel.

As DNA size marker peqGOLD 1 kb DNA-ladder (PEQLAB Biotechnologie GmbH) was used (Figure 12).

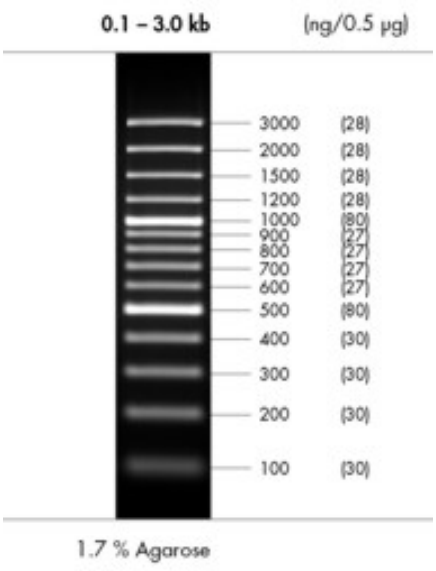

Figure 12. peqGOLD 100 bp DNA-Ladder (PEQLAB Biotechnology GmbH).

The Wizard® SV Gel and PCR Clean-Up System was applied to concentrate PCR reactions and for DNA extractions from agarose gel after electrophoresis.

1.2.6. Morpholino Antisense Oligo- Knock down

Morpholino Oligomeres (Gene Tools, LLC) are chains of several morpholino subunits. Each subunit is made of a ribonucleoside, which was transformed to a morpholino, protected by a trityl- and activated by a phosphoramidate- link. The target sequence can be the mRNA 5' UTR through the first 25 bases of coding sequence (blocking translation initiation in the cytosol), splice junctions or splice regulatory sites (modifying pre-mRNA splicing in the nucleus), mature miRNA or pre-miRNA (inhibiting miRNA maturation and activity) or other cellular RNAs (ribozyme inhibition or translational frameshifting).

Translational knock down is done by sterically inhibition of the formation of the translational initiation complex (Figure 13).

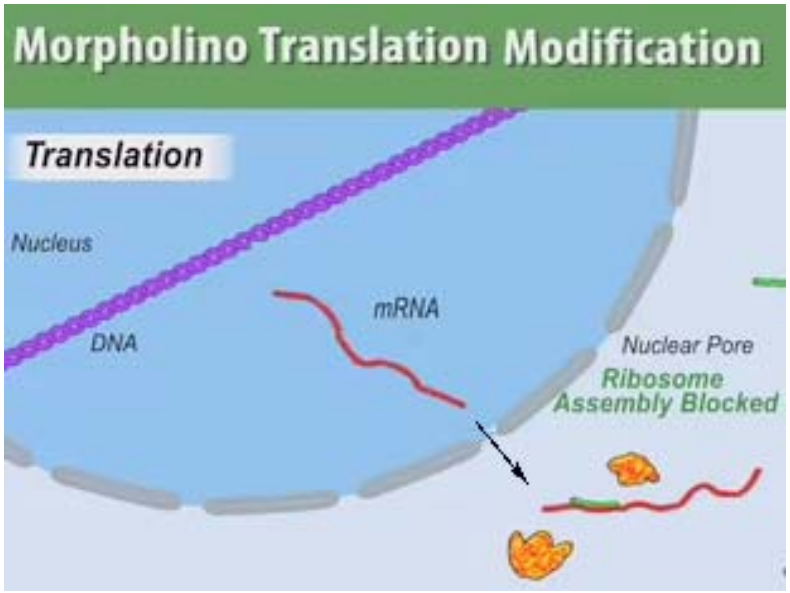

Figure 13. Ribosome assembly is blocked by morpholino (Figure from Gene Tools, LLC, slightly modified).

Morpholinos do not degrade their target and act as RNAse H independent high affinity segment. This implicates that morpholinos action on gene expression cannot be analyzed on RNA level.

It has been shown that Morpholinos have a higher binding affinity than an equivalent DNA-based antisense oligo (http://www.gene-tools.com/) and are therefore capable to give reliable results.

Morpholino delivery can be done by a variety of methods. We decided to choose the Endo-Porter delivery system. It's a novel peptide which delivers substances by an endocytosis-mediated process working in presence of serum, avoiding plasma membrane damage the of the cell. There is no interaction between target and delivery system. The mechanism of delivery is based on endocytosis, mediated by the Endo-Porter, followed by acidification of the endosome. The ionic form of the Endo-Porter permeabilizes the endosome and its content is released into the cytosol (Figure 14).

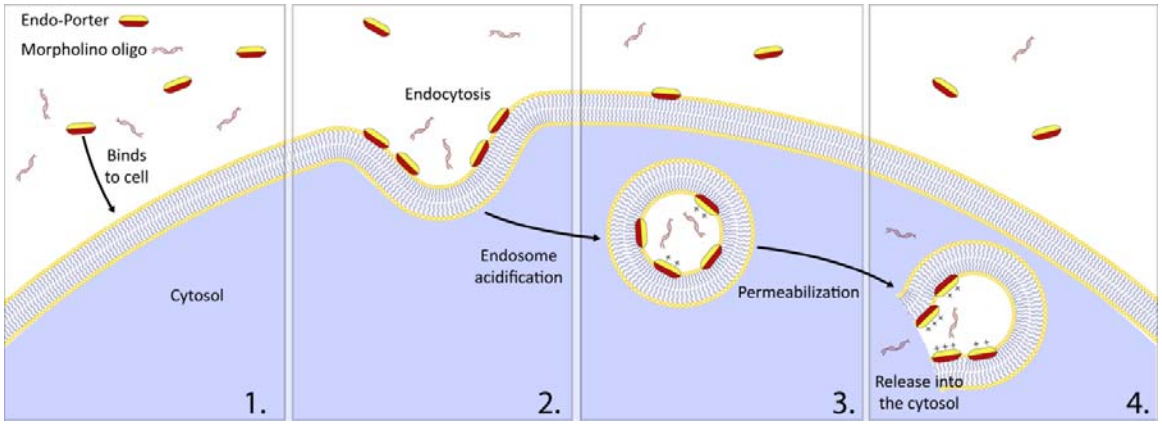

Figure 14. Endo-Porter delivery system: 1.) Endo-Porter's hydrophobic face binds to the cell membrane; 2.) Endocytosis is induced and the Endo-Porter is co-endocytosed along with the morpholinos in the muedim; 3.) Natural acidification of the endosome protonates Endo-Porter that, in its ionic form, permeabilizes the endosome; 4.) Morpholinos are released into the cytosol (Figure kindly provided by Rui Martins).

For our assays, we designed Morpholino oligos targeting the Dscam mRNA (NM_133587.1) using the following sequence:
5′-ACAAGGAGAGAGCCAGTATCCACAT-3′.
Standard control sequence was: 5′-CCTCTTACCTCAGTTACAATTTATA-3′.

Knock down experiments were performed in 6-well plates. Microglia cells from a second shake-off (highest purity) were cultured and treated with 4 µl/ml Endoporter and 5µl/ml Morpholino in microglia medium with reduced serum (see 1.1.1) after about 15 hours. Empty controls and blanks with no Morpholino were also made. Pictures were taken before and 24 hours after treatment. We differentiated 5 morphological states (A: dead, B: amoiboid, C:

bipolar, D: long-processed, E: multipolar) in microglia cells and counted them as shown in as shown in Figure 15 and Figure 16.

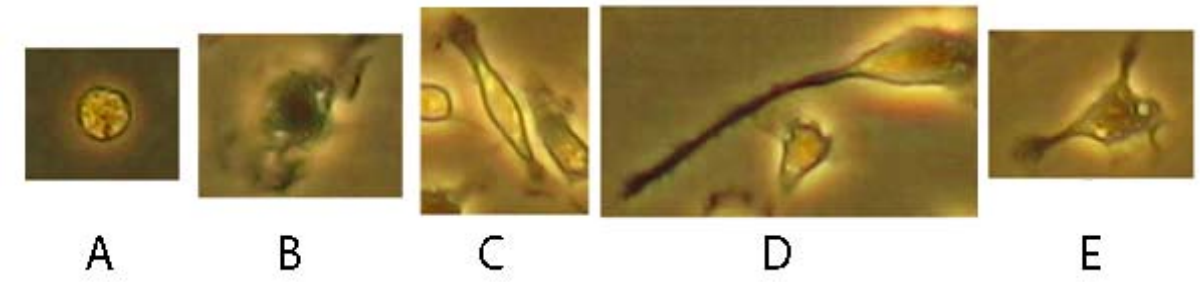

Figure 15. The five different morphological states of microglia cells (A: dead, B: amoeboid, C: bipolar, D: long-processed, E: multipolar).

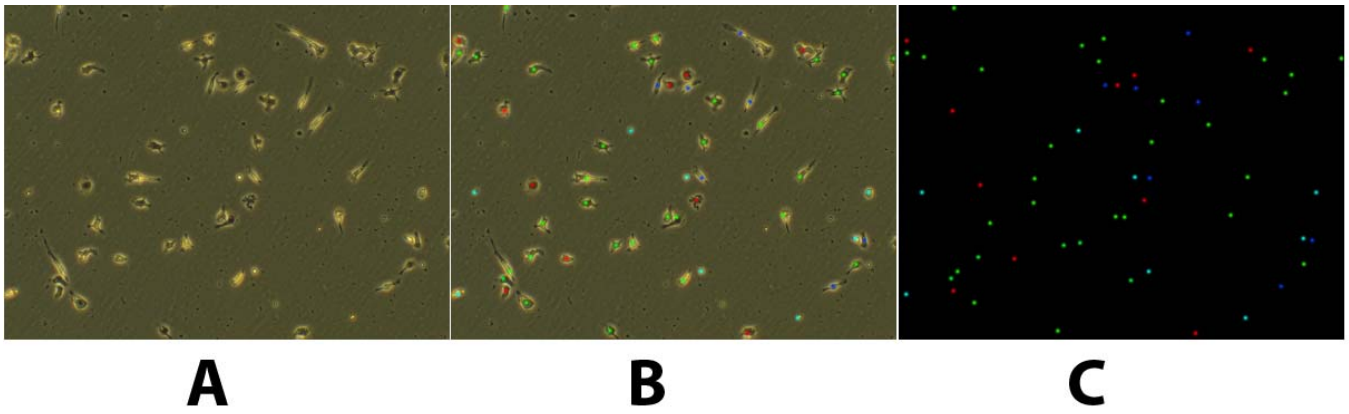

Figure 16. Morphology analysis of morpholino-treated cells. A, unmarked original photo, B marked cells (dead cells = turquoise, amoeboid cells = red, bipolar cells = blue, multipolar cells = green, long-processed cells = purple), C, dots for counting on black background.

1.2.7. Western blot

Protein from second- shake-off- microglia and rat brain protein as positive control were used for western blotting.

1.2.7.1. Protein isolation

Protein was isolated after washing the microglia cells with PBS at RT two times. 1 ml of Lysis buffer (one Protease Inhibitor Cocktail Tablet, Roche Applied Science, in 10 ml 1X RIPA lysis buffer, Pierce Biotechnology, Inc.) was added to the cell pellet from shake off,

completely lysed by pipetting and centrifuged for 15 min at 4 °C and 1400·g. The supernatant containing the whole protein was then transferred into a new 1,5 ml eppendorf tube.

Protein measurement was done with the BCA assay kit (Pierce Biotechnology, Inc.). Total protein was precipitated by adding 500 µl Methanol p.A. and 250 µl Chloroform p.A. (Merck, KGaA) to 500 µl of each sample, and mixed by vortexing briefly. Centrifugation for 5 min at 10000·g at RT followed and the phases were carefully separated with a micropipette. 1000 µl Methanol p.A. were added, vortexed to mix the phases and centrifuged again at for 30 min at 10000·g at 4 º C. Finally, the supernatant was removed, the tube was centrifuged one more time for 10 min at 10000·g at 4 ºC and the pellet was allowed to air-dry at RT after removal of the remaining liquid.

The pellet was then dissolved in 1X NuPAGE® Lithium Dodecyl Sulfate sample buffer (LDS buffer; Invitrogen™), 1X NuPAGE® Reducing Agent (Invitrogen™) to a final protein concentration of 1 to 1,5 µg/µl. The sample was then incubated at 70 ºC for 10 min and spun down for 2 min before finally loading.

1.2.7.2. Protein Electrophoresis

SDS- Page (sodium dodecylsulfate polyacrylamide gel electrophoresis) was performed to separate the proteins. A 5 % stacking and a 10 % separating gel were used (composition v/v, Table 3):

	5% stacking gel	10% separating gel
4X Separating/Stacking Buffer (1,5 M Bis-Tris; pH 6,4)	25%	25%
30% Acrylamide/Bis (Bio-Rad® Laboratories)	33%	17%
10% SDS (Sigma-Aldrich®)	1%	1%
Milli-Q® Water (Millipore™)	40%	56%
TEMED (Electran, BDH)	0,1%	0,1%
10% ammonium persulfate (APS; Amersham® Biosciences, GmbH)	*1%*	*1%*

Table 3. Stacking- and separating- gel recipe for SDS-Page.

For both gels ammonium persulfate was immediately added before casting, as it is the radical initiator for the gelation of the gel. The NOVEX® Gel Cassette (Invitrogen™) (precooled to 4 °C) was used for gel casting.

First, the separating gel was prepared and poured into the chamber and 0,1 % SDS was layered on top. After about 4 hours of polymerization, the 0,1 % SDS was discarded and the gel was washed with 1X stacking buffer (0,5 M Bis-Tris; pH 6,4). Any remaining liquid was aspirated by a vaccum pump.

Secondly, the stacking gel was mixed and cast on top of the separating gel. The comb was carefully put into the liquid gel, avoiding any bubbles, and the stacking gel was allowed to polymerize for 30 min. Then the comp was removed carefully and the slots were rinsed with stacking buffer to remove barely fixed gel remains.

The gel assembly was then placed into the electrophoresis unit (Bio-Rad® Laboratories), 1X MOPS buffer was prepared and NuPAGE® Antioxidant (Invitrogen™) was added to a final concentration of 0,25 % (v/v). 1X MOPS running buffer was poured into the inner chamber and the remainder was put into the outer chamber. Samples were loaded next to MagicMark™ Western Protein Standard (Invitrogen™) and the gel was run at a constant voltage of 200 V and about 130 mA for 45 min.

1.2.7.3. Immunoblot

The cassette was disassembled, the stacking gel was discarded and the separating gel was equilibrated in transfer buffer (Tris 479 mM; Glycine 386 mM; 0,5% SDS; 10% Methanol; Milli-Q® Water) for 15 min. A commensurate Immobilon-P Polyvinylidene fluoride Membrane (PVDF; Millipore™) membrane was equilibrated by dipping in methanol p.A. for 15 sec and Milli-Q® Water (Millipore™) water for 2 min and then also placed in transfer buffer for 10 min. The immunoblot was set up as shown in Figure 17 and run for about 60 min at 20 V.

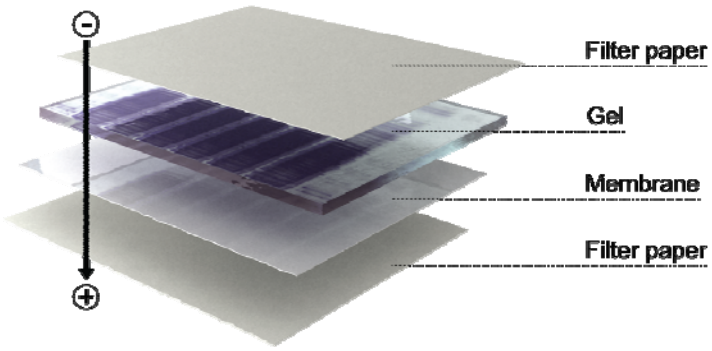

Figure 17. Immunoblot setup (Figure kindly provided by Rui Martins).

When the transfer was finished, the membrane was blocked in blocking buffer (1,5 % w/v Non-Fat Dry Milk powder in PBS; 0,1 % TWEEN-20) for 1 hour. The membrane was cut in two pieces and each incubated with one primary antibody, goat anti-human Dscam and mouse anti rat β-actin (see 1.3.1). They were diluted 1:500 in blocking buffer and incubated at 4 °C over night on a shaker.

The following day, the membrane was washed three times for 15 min with blocking buffer and then incubated with a 1:2000 dilution of the secondary antibody, Alkaline Phosphatase-conjugated donkey anti-goat IgG/Alkaline Phosphatase- conjugated goat anti-mouse IgG (see 1.3.10) in blocking buffer for one hour at RT. The three washings in bocking buffer were repeated with additional 3 washings in assay buffer (25 mM Diethanolamine - Fluka® Analytical; 1 mM $MgCl_2$; Milli-Q® Water; pH 10,0), 5 minutes each.

The detection was done with CDP-Star® Reagent (New England Biolabs, Inc.) as substrate. Assay buffer was mixed with 10 µl of the substrate and incubated for 2 min with the membrane, placed between two plastic foils. The results were captured using a Fluor-S™ Imager (λ = 290-365 nm; Bio-Rad Laboratories).

1.2.8. Northern blot

RNA was isolated (see 1.2.1) from CD-45^{low} FACS-sorted microglia and from spinal cord as positive control.

1.2.8.1. RNA Electrophoresis

RNA tends to bind other RNAs and can easily form secondary structures. This would modify the running speed in electrophoresis. So, a denaturizing formaldehyde gel is used to prevent this process.

For preparation of 10x MOPS buffer 0,2 M MOPS (4-**Mo**rpholine**p**ropane**s**ulfonic acid, Sigma-Aldrich®) 0,05M sodium acetate and 0,01 M EDTA were mixed and adjusted to pH 7,0 with 1 M sodium hydroxide.

Agarose (1% w/v) was mixed with water and nuked to the boil. After cooling to about 60 °C, 10x MOPS buffer (to a final concentration of 1x) and 37% formaldehyde (Sigma-Aldrich®, to a final concentration of 7%) were added and the gel was cast. The tray, comb and tank were cleaned with soap, washed with RNAse-free water and dried before use.

The RNA sample (minimum of 1 µg total RNA, measurement by NanoDrop™ analyzer) was mixed with 10X MOPS (to a final concentration of 1x), 37% formaldehyde (to a final concentration of 6,5% w/v) and formamide (to a final concentration of 50% v/v), incubated at 60°C for 5 min, mixed with loading buffer and run on the gel for about 4 hours at 60 V. 1X MOPS buffer was used as running buffer.

1.2.8.2. Blotting

The gel was washed with water two times and placed in 10x SSC buffer for 45 min with shaking. The nylon membrane was soaked in water and 20x SSC (3M sodium chloride, 3 mM sodium citrate, brought to ph 7.0 with HCl)

Then the blotting setup was done as shown on in Figure 18 over night.

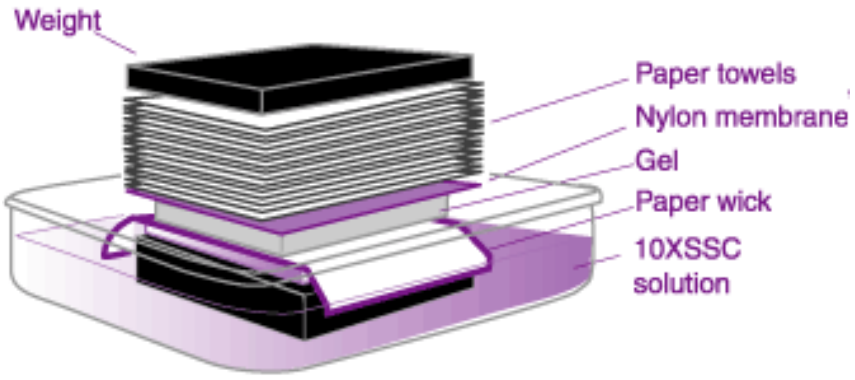

Figure 18. Northern blot setup (Figure taken from http://www.biochem.arizona.edu/).

After this the membrane was crosslinked by a Stratalinker® UV Crosslinker (Model 1800, #400072). Prehybridization at 55°C for 4 hours and hybridization at 55°C over night followed. Buffers were prepared as listed in Table 4. The hybridization probe (minimum of 100 ng, measured by NanoDrop™ analyzer) was prepared as described in 1.2.3.

Substances	**Prehybridization buffer**	**Hybridization buffer**
Formamide	50%	50%
100x Denhardts solution (each 0,2% w/v BSA, Polyvinilpyrolidone and Ficoll in water	5x	2,5x
20% SDS	1%	1%
10 mg/ml salmon sperm DNA	200 µg/ml	200 µg/ml
20x SSPE (3 M sodium chloride, 200 mM sodium dihydrogen phosphate, 200 mM EDTA in water, adjusted to pH 7.4)	5x	5x
Water		

Table 4. Hybridization buffer recipes for Northern blot.

After hybridzation, three washing steps with 1x SSPE, 0,1% SDS at 55°C for 20 min and one with 0,1x SSPE, 0,1% SDS at RT for 50 min were performed. Last, the substrate was mixed and incubated for 20 min at RT.

Detection was done using NBT/BCIP (Roche Applied Science) according to the manufacturer's instructions.

1.3. Immunochemistry

1.3.1. Antibodies

Antibodies were used for FACS, Western blot, Ultramicroscopy and tissues.

For some approaches, it was necessary to permeabilize the cells. This was performed with FIX&PERM® kit (Invitrogen™) according to manufacturer's instructions. All antibodies used were kept at 4º C and protected from light.

Table 5: Antibodies

Name	Recognizes	Company	Use
Texas Red labeled Lycopersicon Esculentum (Tomato) Lectin	lectin sugar moieties	Vector Laboratories	Ultramicroscopy
Monoclonal human 5D4	Human Keratansulphate proteoglycan	Seikagaku Corporation	FACS
Polyclonal goat anti-human DSCAM	Human DSCAM extracellular domain	R&D systems	FACS IHC WB
Cy™5-conjugated* AffiniPure Donkey Anti-Goat IgG (H+L)	Goat IgG	Jackson ImmunoResearch	FACS IHC
Biotin-SP-conjugated AffiniPure Bovine Anti-Goat	Goat IgG	Jackson ImmunoResearch	IHC
Cy™5-conjugated Streptavidin	Biotin	Jackson ImmunoResearch	FACS IHC
FITC- conjugated monoclonal mouse CD45	Rat thymocyte membrane glycoproteins	AbD Serotec	FACS
FITC- conjugated monoclonal anti-rat CD11b	Rat CD11b	AbD Serotec	FACS
PE-conjugated polyclonal donkey anti-goat IgG H&L – F(ab)2 fragment	Goat IgG whole molecule	abcam®	IHC
Biotin-SP-AffiniPure F(ab')2 Frag Anti-Goat IgG	Goat IgG	Jackson ImmunoResearch	IHC
Avidin-Peroxidase	Biotin	Sigma-Aldrich®	IHC
Mouse anti-rat CD11b	Rat CD11b	AbD Serotec	IHC
Anti mouse AP	Mouse IgG	Jackson ImmunoResearch	IHC
Rabbit anti-Iba1	Human, mouse, rat Iba1	WAKO	IHC
Alkaline Phosphatase-conjugated goat anti-rabbit IgG	Rabbit IgG	Jackson ImmunoResearch	IHC

Mouse monoclonal anti β-actin	Hu, Ms, Rat, Cat, Chk, Cow, Dog, Fsh, Gpig, Hm, Mmst, Op, Pig, Rb, Shp β-actin	abcam®	WB
Alkaline Phosphatase-conjugated AffiniPure F(ab') 2 Fragment Donkey Anti-Goat IgG	Goat IgG	Jackson ImmunoResearch	WB
Goat polyclonal to Mouse IgG (Fc specific) (Alkaline Phosphatase)	Mouse IgG	abcam®	WB

1.3.2. Flow cytometry analysis and cell sorting

Cells from isolation of the microglia from the crude CNS preparations (described in 1.1.5), cells from shake-off or from cold shock- detached cell culture plates were used for FACS or flow cytometry analysis. The cell suspension was centrifuged for 1 min/ml at 1400·g and the pellet was resuspended in about 200 µl stain buffer. BD Pharmingen™ stain buffer was used through staining procedures and all antibodies were offered at 4 °C or RT and for 30 min. Each staining was followed by washing with 1-3 ml stain buffer and 10 minutes centrifugation at 4 °C or RT, at 1400·g.

Fluorescence associated cell sorting (FACS) was performed using the FACSAria II cell sorter with the FACSDiva™ (Becton Dickinson) software at the St. Anna Kinderspital. A 70µm wide nozzle was used for sorting, and it was performed according to Forward Scatter (FSC, quantifying size/viability), Side Scatter (SSC, quantifying granularity) and relative CD45/5D4 labeling (see 2-3-1) as parameters. The sorted cells were collected in tubes containing 350µL RLT lysis buffer (Quiagen RNeasy kit®) with 3,5µL β-Mercaptoethanol. Then the lysed cells were stored at -80ºC, or immediately processed for total RNA isolation (see 1.2.1).

Flow cytometry analysis was performed with different antibodies (see 1.3.1). For some approaches the cells have been treated with FIX&PERM® kit (Invitrogen™) to stain intracellular proteins.

1.3.3. Histological/Cytoblock Staining

Histological analysis was performed as previously described (Aboul-Enein et al., 2004): The animals were perfused with 4% paraformaldehyde (PFA) in phosphate buffered saline (PBS), brains and spinal cords were dissected, fixed in 4 % PFA/PBS for 24 hours and paraffin embedded. 2-4 µm thick adjacent serial sections were cut on a microtome.

Prefixed microglia (PFA) cells from shake-off were embedded in 1 % low melting agarose (now referred as cytoblock), cut on a microtome and stained equally.

Antigen retrieval of the Tissue/Cytoblock sections was done by rehydrating, heating in citrate buffer, rinsing in 0,1 M PBS and then incubation in PBS containing 10% fetal calf serum (PBS/FCS) for 20 minutes. After this another washing step with PBS follwed. Pretreatment with 0,2 % hydrogen peroxide (blocking endogenous peroxidase) was followed by addition of the primary antibodies goat anti-human Dscam (1:250) and rabbit anti-rat Iba1 (1:3000), and incubated over night at 4 °C. Anti-rat ionized calcium-binding adapter molecule 1 (Iba1) is specific for macrophages/microglia (Jones and Tuszynski, 2002).

The sections were then washed in PBS and incubated with the secondary antibodies biotin conjugated bovine anti-goat (1:200) and alkaline phosphatase- conjugated goat anti-rabbit (1:200) in PBS/FBS at room temperature for 1 hour. AP-conjugated antibody was followed by a peroxidase-conjugated avidin (1:200) for another hour. Detection was done with 3,3'-diaminobenzidine-tetra-hydrochloride (DAB, Sigma-Aldrich®) containing 0,01 % hydrogen peroxide for peroxidase and/or Fast red (Sigma-Aldrich®) for alkaline phosphatase. Brain sections were counterstained with Mayer's Hämatoxylin. See 1.3.1 for antibody details. The complete stained sections were dehydrated and coverslipped.

1.3.4. Immunostaining of mixed glia cell culture plates

The cells were stained with DAB (DAB, Sigma-Aldrich®)/Fast Red or Cy3/FITC in culture plates with and without permeabilization. 350 µl of DAKO buffer (light microscopy), stain buffer (fluorescence microscopy) or microglia medium (before fixation) was used for staining procedures. Fixation was done by the FIX&PERM® kit (Invitrogen™) or by methanol/hydrogen peroxide after primary antibodies.

Light microscopical staining were performed with goat anti-human Dscam (1:30)/biotin anti-goat (1:100)/avidin- peroxidase (1:100) and mouse anti-rat CD11b (1:100)/anti-mouse-

alkaline phoshatase (1:100). For fluorescence staining Cy3 anti-goat (1:100) and CD11b-FITC (1:100) was used. For antibody details see 1.3.1.

All antibodies were incubated while shaking for 1 hour at RT in the dark. Detection was done with 3,3'-diaminobenzidine-tetra-hydrochloride (DAB, Sigma-Aldrich®) containing 0,01 % hydrogen peroxide for peroxidase and/or Fast red (Sigma-Aldrich®) for alkaline phosphatase. Finally, the walls of the plates were cut off with a hot scalpel, grinded by a razor and then mounted on big coverslips with geltol/gelate.

2. Results

At the beginnings of my work 5D4^{high} and 5D4^{low} microglia had been characterized and analyzed by microarrays (Ephraem Leitner, diploma thesis, 2008). It was found that the expression levels of many molecules differ dramatically between the two populations. The following 5 molecules were especially interesting for us: *Cadm1, Dlx2, Dscam, Tef, Twist-2;*

These molecules had higher expression levels in 5D4^{high} MG than in their 5D4^{low} counterparts (Table 6).

Full Name	Symbol	Target Id	p-Value	log2Fold Change
Rattus norvegicus cell adhesion molecule 1	**Cadm1**	NM_001012201	0,00046	1,032
Rattus norvegicus distal-less homeobox 2	**Dlx2**	XM_230986	0,04063	1,109
Rattus norvegicus Down syndrome cell adhesion molecule	**Dscam**	NM_133587	0,00208	1,093
Rattus norvegicus thyrotrophic embryonic factor	**Tef**	NM_019194	0,02887	1,034
Rattus norvegicus twist homolog 2 (Drosophila)	**Twist2**	NM_021691	0,00802	1,512

Table 6. Microarray data of target molecules; p-values and log2fold expression in 5D4^{high} relative to 5D4^{low} microglia;

All these molecules might play an important role in microglia development and function:

- *Cell adhesion molecule 1 (Cadm1, Necl-2)* is a ligand for class I MHC-restricted T-cell associated molecule (Crtam) and it was proposed that this molecular pair could regulate a large panel of cell/cell interactions both within and outside of the immune system (Galibert et al., 2005).
- *Dlx2*: Distal-less homeobox transcription factors (Dlx) are involved in lymphocyte development (Sunwoo et al., 2008).
- *Down syndrome cell adhesion molecule (Dscam)* was first described in neuronal development. Recent studies present Dscam in a new context: D. melanogaster immune tissues can express more than 18,000 different extracellular domains of Dscam and soluble forms of Dscam have also been identified in cell supernatants and in the haemolymph. Dscam potentially acts as both a phagocytic receptor and an opsonin. This suggestion is supported by the identification of Dscam in the phagosome proteome of Drosophila. The crystal structures of two Dscam isoforms reveal each one with two distinct surface epitopes, one on either side of the receptor. This configuration allows a given Dscam isoform to form a homodimer

(epitope I) and retain the ability to recognize, opsonize and crosslink pathogens (epitope II) (Stuart and Ezekowitz, 2008).

- *Tyrotroph embryonic factor (Tef)* was found to be one of the apoptotic regulators in hematopoetic progenitors and to control hematopoetic cell proliferation by regulating the expression of cytokine receptor βc chain (Inukai et al., 2005).
- *Twist-2* has been characterized as a critical factor in regulation of myeloid lineages, as well as in function and inflammatory responses of mature myeloid cells (Sharabi et al., 2008).

Microarray data give a first hint at RNA expression, but they have to be confirmed by other techniques. Therefore, I first tried to confirm these findings by PCR.

2.1. MG express Dlx2, Dscam, Tef and Twist-2 mRNA

I isolated cDNA from a 2nd microglia shake-off, which is known to contain the purest microglia population, and used it for PCR with primers (see Table 2. Primer-sequences and melting temperatures.) specific for the five target genes and GAPDH as control, resulting in qualitative information about expression of Cadm1, Dlx2, Dscam, Tef and Twist2 mRNA transcripts. This sample was used to get information about the whole microglia population. Defined, sorted populations were used in further steps.

Four out of five target genes could be confirmed by PCR: Dlx2 (two bands at 211 bp and ~1 kb), Dscam_small (one band at 269 bp), Tef (one weak band at 238 bp) and Twist2 (one band at 293 bp), while Cadm1 products were missing (Figure 19).

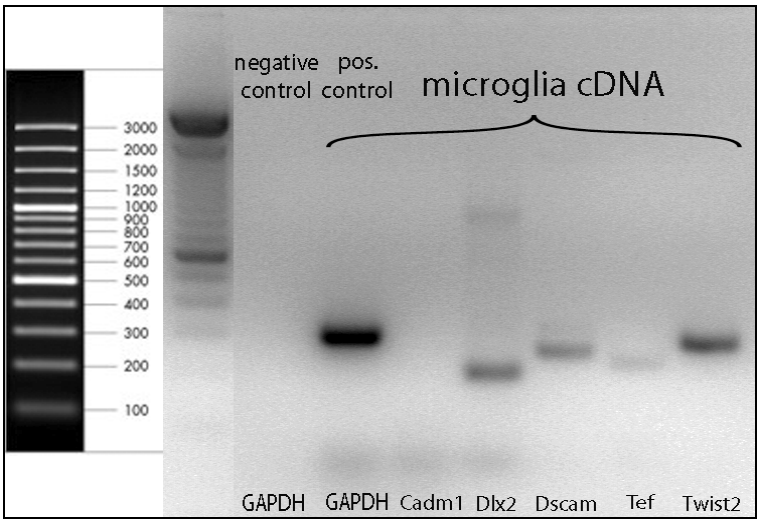

Figure 19. Gelelectrophoresis of GAPDH (310 bp), Cadm1 (105 bp), Dlx2 (211 bp), Dscam (269 bp), Tef (238 bp), Twist2 (293 bp) PCR products. cDNA from pure shake-off microglia was used.

PCR products from Dlx2, Dscam_small, Tef and Twist2 were purified (see 1.2.1) for further confirmation by sequencing. The upper 1 kb product (Dlx2) could not be detected by sequencing with Dlx2 primers. All products had a >98% sequence identity to their targets:

Primer used for sequencing	**Identities product/target**
Dlx2 Fwd	182/182 (100,0%)
Dlx2 Rev	177/177 (100,0%)
Dscam_small Fwd	238/238 (100,0%)
Dscam_small Rev	129/131 (98,5%)
Tef Fwd	205/205 (100,0%)
Tef Rev	204/207 (98,6%)
Twist2 Fwd	208/211 (98,6%)
Twist2 Rev	262/263 (100,0%)

Table 7. Blast results of the found PCR- product sequences.

For the rest of my studies, I concentrated on Dscam. Since Dscam is an extremely long protein, and since its RNA is subject to extensive splicing, we selected additional primes for further studies. Their positions are illustrated in Figure 20 and listed in Table 8:

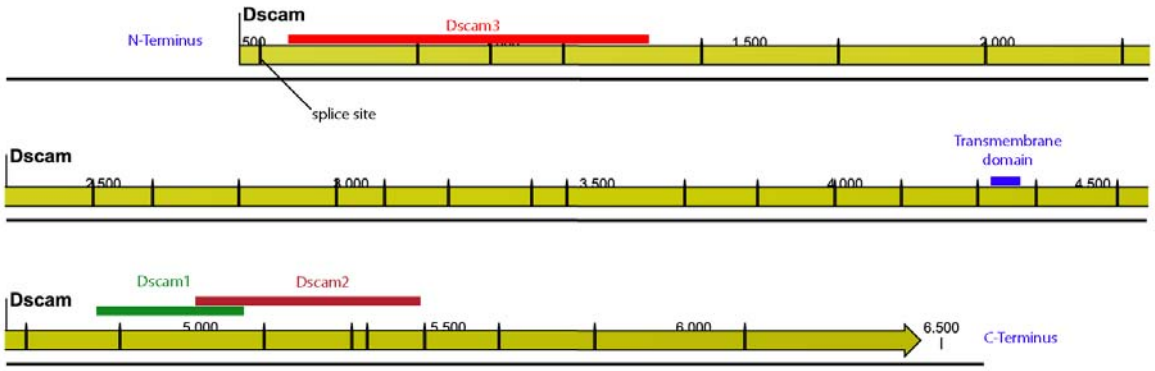

Figure 20. Dscam (NM_133587), including annotated Dscam PCR- product positions

	Fwd	Rev	Length
Dscam_small	4853-4873	5100-5121	268 bp
Dscam_middle	4988-5007	5486-5505	517 bp
Dscam_large	537-560	1239-1262	726 bp

Table 8. Dscam primer positions and PCR- product lengths.

These primers were used to further confirm the presence of Dscam transcripts in microglia cells:

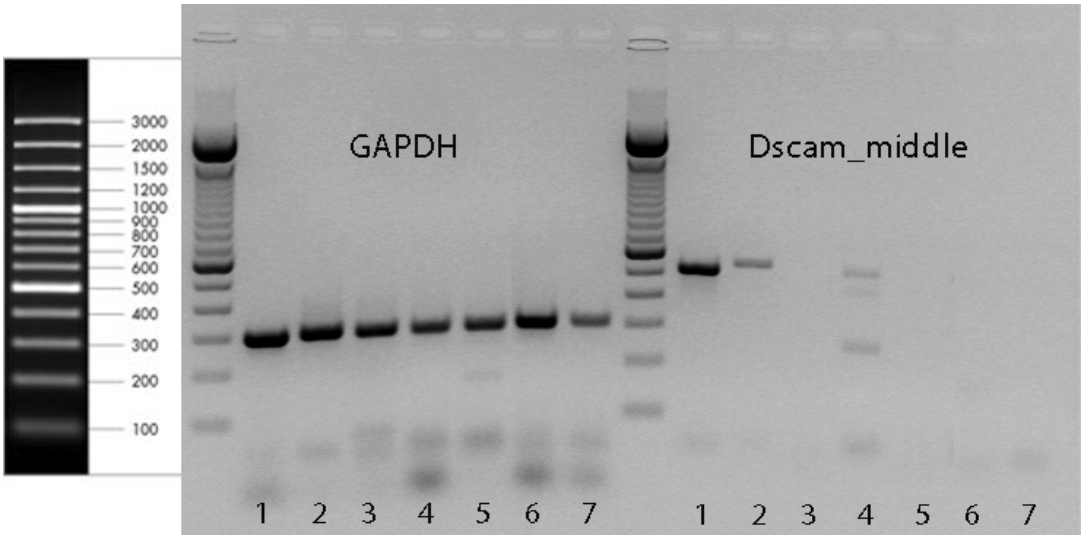

Figure 21. Gelelectrophoresis of GAPDH (310 bp, pos. control) and Dscam_middle (517 bp) PCR products. Dscam transcripts were found in microglia from 2nd shake-off (1) and CD45-low cells from healthy adult rat spinal cords (2) and PLP transgenic adult rat spinal cords (4), whereas CD45-high cells from healthy adult rat spinal cords (3) and PLP transgenic adult rat spinal cords (5) and macrophages from peritoneum (6) and spleen (CD45-low sort) (7) appeared to be Dscam-negative.

Dscam_middle (517 bp) was detected in microglia from the 2nd shake off and in sorted microglia ($CD45^{low}$) from healthy and PLP transgenic rat spinal cords by PCR. $CD45^{high}$ cells from spinal cord- sorting and macrophages from peritoneum or spleen ($CD45^{high}$ sorted) appeared to be Dscam negative.

We were also able to obtain PCR products from the N- termius of Dscam, using the Dscam_large primers, which yielded a product in the expected range of 821 bp.

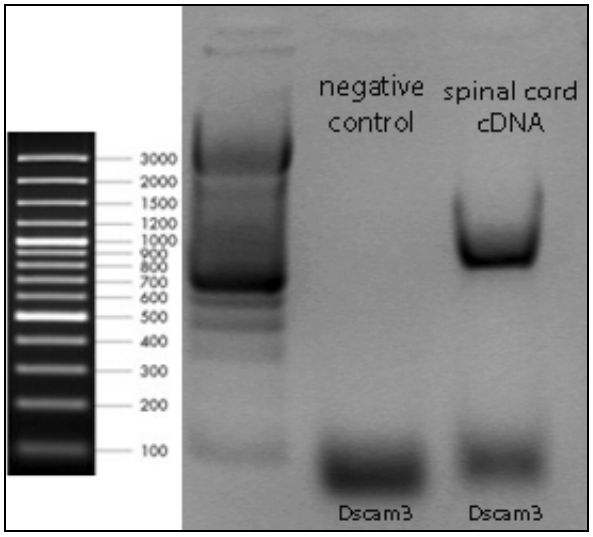

Figure 22. Gelelectrophoresis of Dscam_large- PCR product (821 bp). The transcript was found in microglia from the 2nd shake off.

Cumulatively, these data strongly suggested that MG, but not macrophages express Dscam transcripts. Do they also make Dscam protein?

2.2. Microglia cells express Dscam protein

To study the expression of Dscam protein, we used total protein from rat microglia from the 2nd shake off and from rat brain (as control) for Western blotting with Dscam and β-Actin antibodies (see 1.3.1). Two western blots were performed, both resulting in a ~100 kDa weak band for Dscam in rat microglia and rat brain total protein (Figure 23). This was surprising, since rat Dscam protein should be in the range of 222,3 kDa (reported sequence in the NCBI database (National Center of Biotechnology Information)) and since the β- actin band was in the expected range of 41,7 kDA.

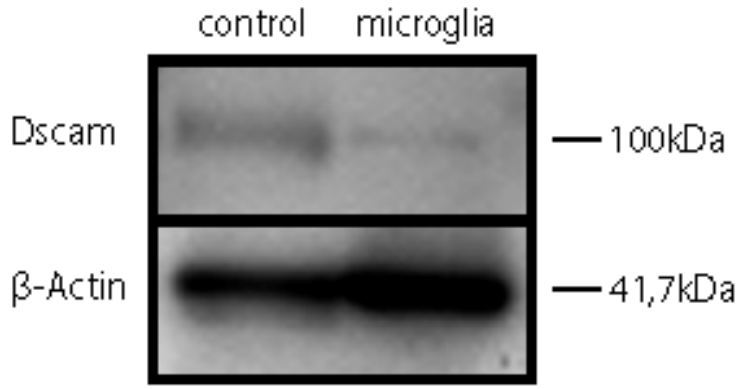

Figure 23. Dscam/β-Actin Western Blot of microglia/rat brain protein.

We therefore decided to analyze Dscam protein expression in MG by two additional techniques: by immunocytochemical stainings and flow cytometry analysis

2.3. Immunological Stainings

2.3.1. Stainings of brain sections

Our antibody available for these stainings has initially been raised in goats against human Dscam, and it has been described to bind to mouse Dscam as well (Fuerst et al., 2008). In a first step, we wanted to prove that this antibody is also useful for the detection of rat Dscam. For this purpose, we found a weak reactivity of many different neurons and a very strong reactivity of neurons in the facial motor nucleus and in the cochlear nucleus (Figure 24, adapted from Paxinos and Watson, 2007, and Figure 25).

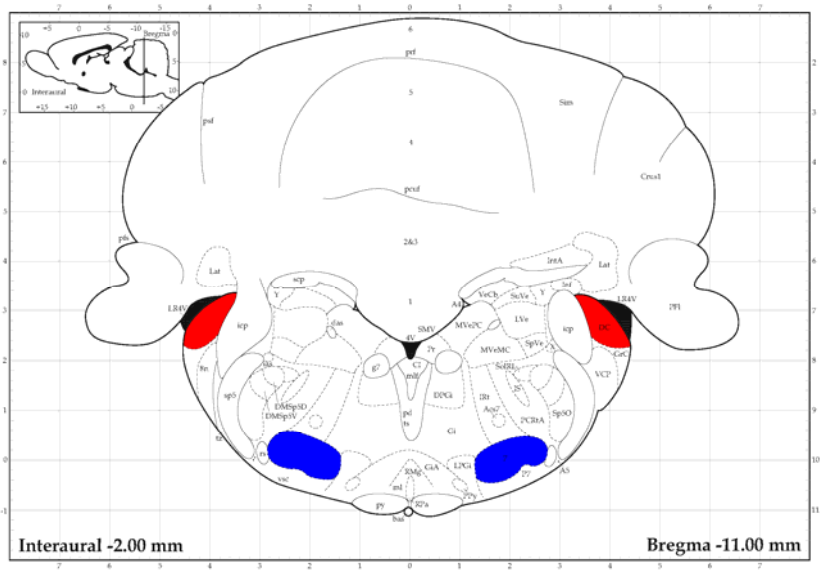

Figure 24. Facial nuclei (blue) and cochlear nuclei (red) of a rat brain section (-2,0 mm interaural, -11,0 mm bregma, adapted from Paxinos and Watson, 2007).

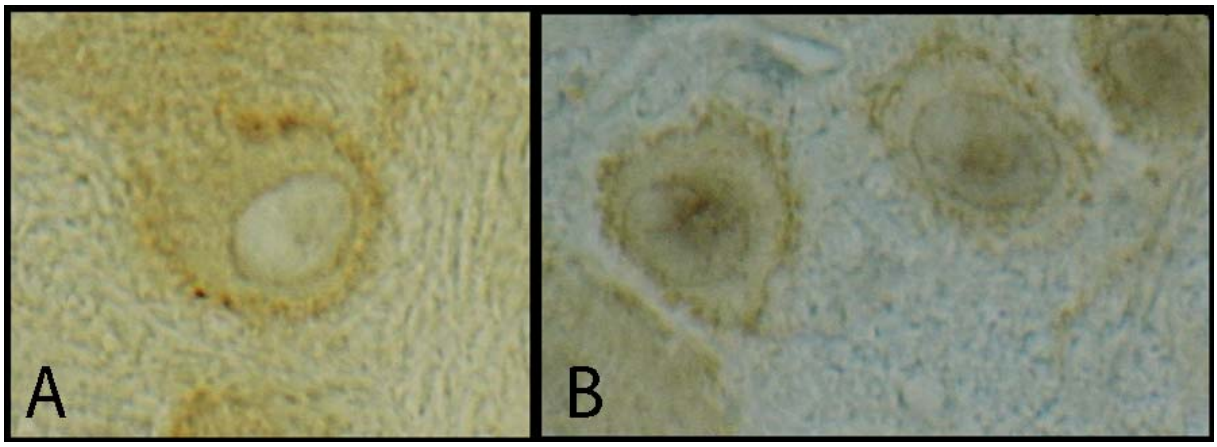

Figure 25. Immunocytochmical staining of brain sections with Dscam. (A) Motor neurons from facial nucleus (100X); (B) Neurons from cochlear nucleus (100X);

We did not see Dscam positive cells with this staining procedure, which could indicate that these cells express much lower levels of Dscam than neurons. To analyze whether we are able to obtain a stronger Dscam reactivity on MG in vitro, I next used mixed glia culture monolayers for immunocytochemistry.

2.3.2. Stainings of mixed glial cell culture monolayers

These mixed glia culture contain MG on top of an astrocyte/fibroblast feeder layer. To unequivocally identify MG, thes cultures were double stained with mouse anti-rat CD11b and with goat anti-human Dscam antibody.

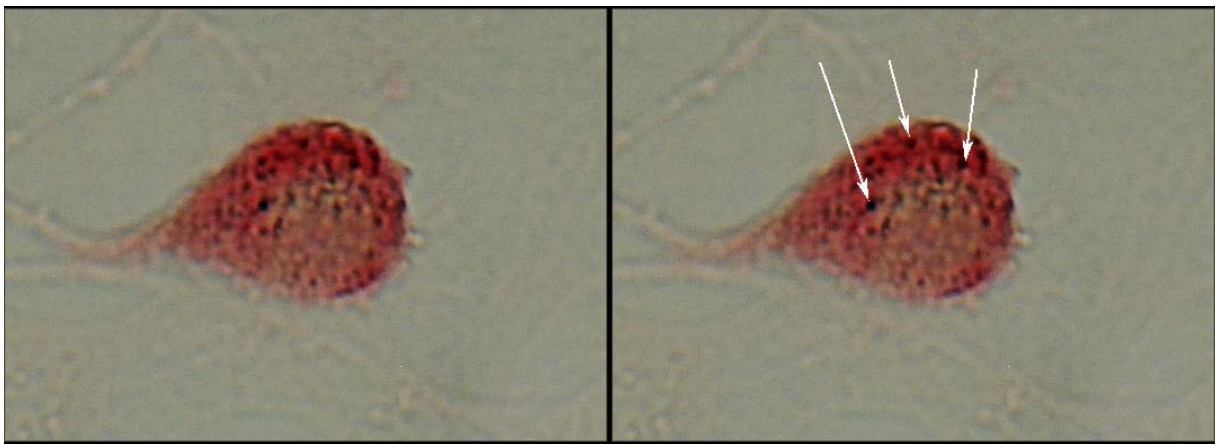

Figure 26. Dscam/CD11b double staining of mixed glial cell cultures (100X). A CD11b positive cell is stained in red. Please note the presence of punctuate, black Dscam reactivity in this cell (arrows).

The number of CD11b/Dscam double positive cells in the total CD11b positive MG pool was exceedingly low. Only 3-5 of these double positive cells were found in a 50 mm petri dish.

2.3.3. Analysis of pure microglia cells

Parallel to these studies on mixed glia cell culture monolayers, I also analyzed pure microglia. I embedded clean shake-off (2^{nd}) microglia cells in low melting agarose and cut the block like rat brain into 4 µm sections on a microtome. Microglia cells were stained with Iba1 and Dscam antibodies. Anti-rat ionized calcium-binding adapter molecule 1 (Iba1) is specific for macrophages/microglia (Jones and Tuszynski, 2002). Under these conditions, many Dscam/Iba1 double positive cells were found. Approximately 10 % of all Iba1 positive cells were also positive for Dscam (Figure 27).

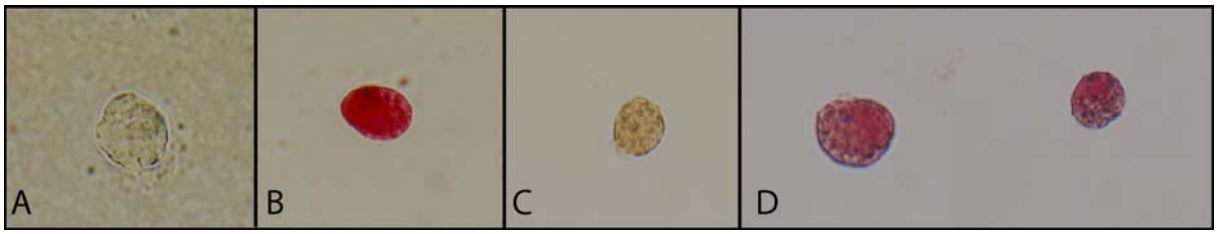

Figure 27. Dscam/Iba1 stainings of cytoblock sections. Iba 1 reactivity is shown in red, Dscam reactivity in black. (A) Negative control. (B) -/Iba1. (C) Dscam/-. (D) Dscam/Iba1. (Phase contrast, 100X)

Admittedly, all the data presented so far was rather "soft": They hinted at an expression of Dscam in MG, but were far from convincing. To further improve this, I next tried to enhance the sensitivity of detection in FACS analysis.

2.4. Fluorescence associated cell sorting

2.4.1. Dscam flow cytometry

To detect surface expression and intracellular expression of Dscam, the cells were analysed in the absence or presence of permeabilization, respectively. Unfortunately, all 9 FACS analyses performed were essentially negative. I just show one example underneath (Figure 28).

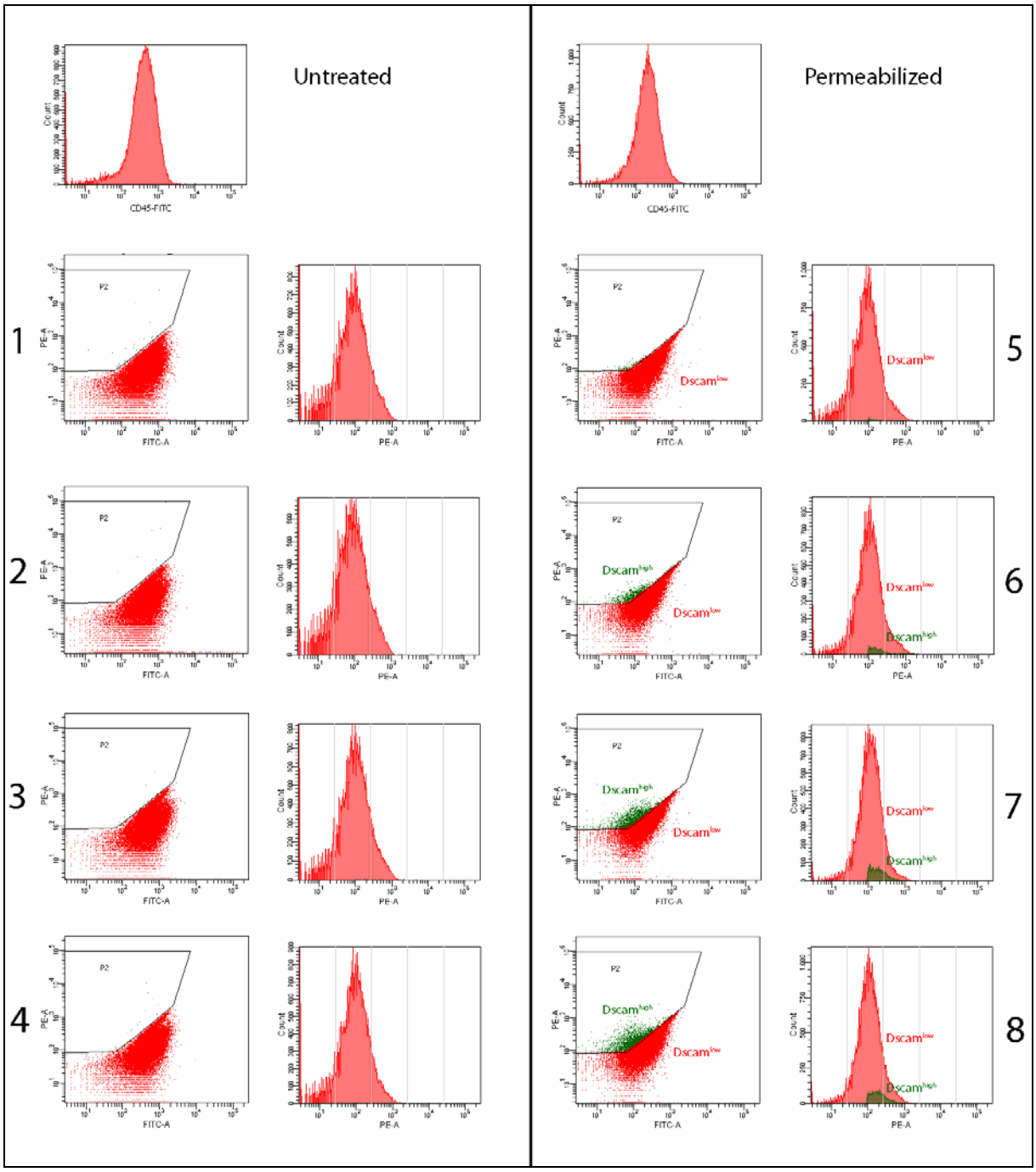

Figure 28. Dscam/CD45- Flow cytometry analysis with untreated and permeabilized microglia cells (2nd shake-off). Dscam was detected by PE- conjugated donkey anti-goat. All antibodies were incubated for 30 min at 4°C. The diagram on the top shows that I analyzed a uniform population of CD45 positive MG cells. Untreated (1-4) and permeabilized (5-8) cells were investigated with different Dscam antibody dilutions: negative control (1, 5), 1:50 (2, 6), 1: 20 (3, 7), 1:4 (4, 8); PE- conjugated donkey anti-goat and CD45-FITC were used 1:100;

Since all other attempts to verify protein expression in living cells were unsuccessfull, and since we were afraid that these negative results were caused by the usage of an antibody which could be suboptimal for the detection of rat Dscam, we decided to use the most

sensitive technique of all: a biological read-out for the detection of a functional Dscam in rat MG cells.

2.5. Knock down experiment

We decided to study the function of this protein in knock-down experiments, using a system based on the Endoporter mediated delivery of morpholinos (see 1.2.6). The procedure of this essay is illustrated in Figure 29.

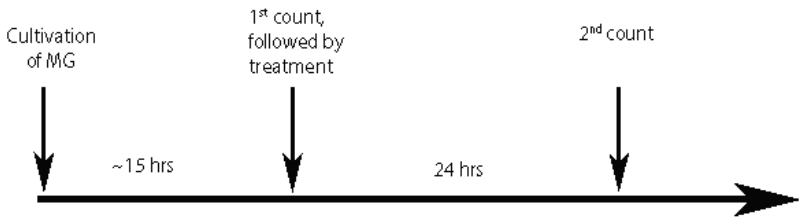

Figure 29. Endoporter/Morpholino treatment procedure.

MG attached well after 15 hours, and a roughly constant distribution of morphological states developed (Figure 30). Morphological changes were noticed 24 hours after treatment with Endoporter and Morpholino (Figure 30).

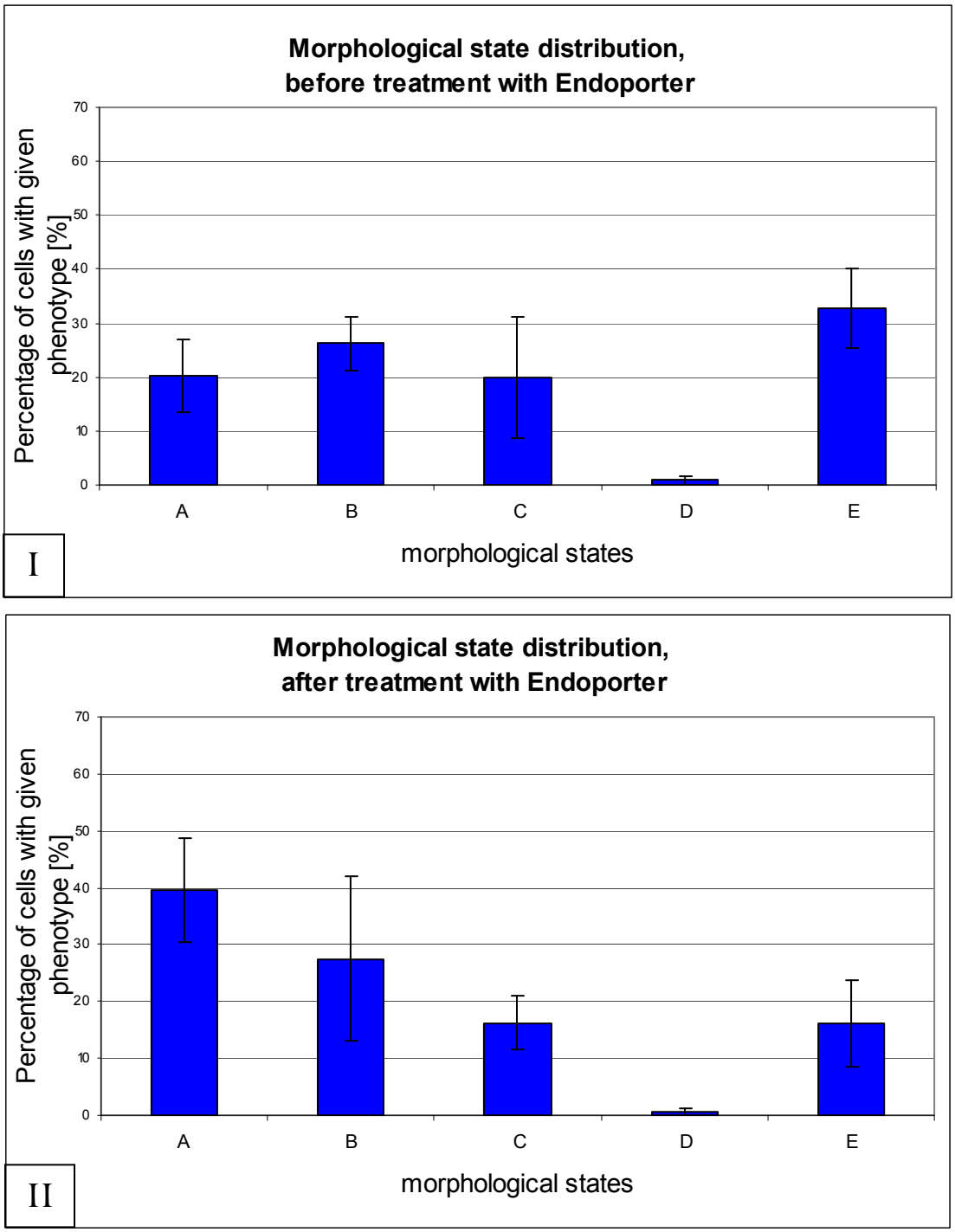

Figure 30. Cell state distribution before and 24 hours after treatment with Endoporter and Morpholino; combined data from two representative studies. (A: dead, B: amoeboid, C: bipolar, D: long-processed, E: multipolar)

To give a better overview of these two charts, the proportional change of each morphological state due to Endoporter/Morpholino treatment is shown underneath (Figure 31).

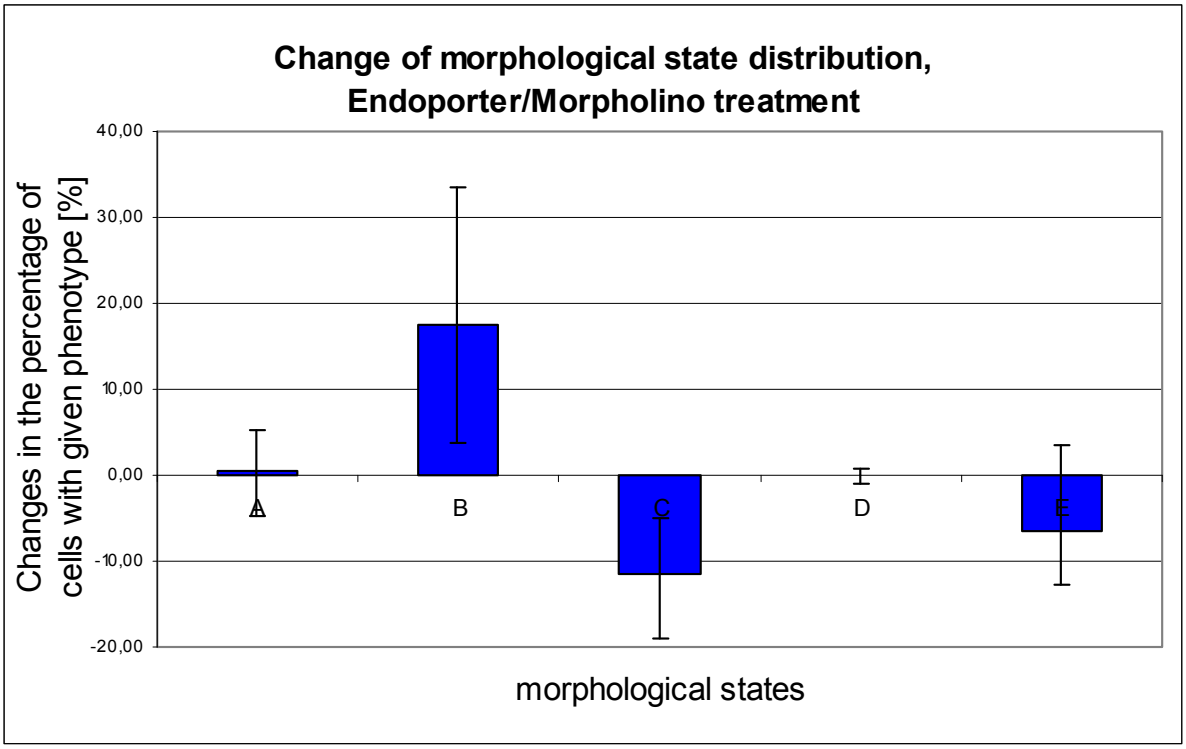

Figure 31. Change of morphological cell state distribution from before treatment to 24 hours after treatment with Endoporter and Morpholino; combined data from two representative studies. (A: dead, B: amoeboid, C: bipolar, D: long-processed, E: multipolar)

Increased numbers of amoeboid cells and decreased numbers of bipolar and multipolar cells could be observed by this treatment. Interestingly, the increased population has a phagocytic phenotype.

Since the delivery of Morpholinos by the Endoporter depends on phagocytosis, there was the risk that these changes in phenotype were caused by the action of the Endoporter itself. Therefore we also tested the action of Endoporter only. We found that Endoporter leads to an increase in apoptotic cells, but did not cause an amoeboid phenotype (Figure 32, Figure 33).

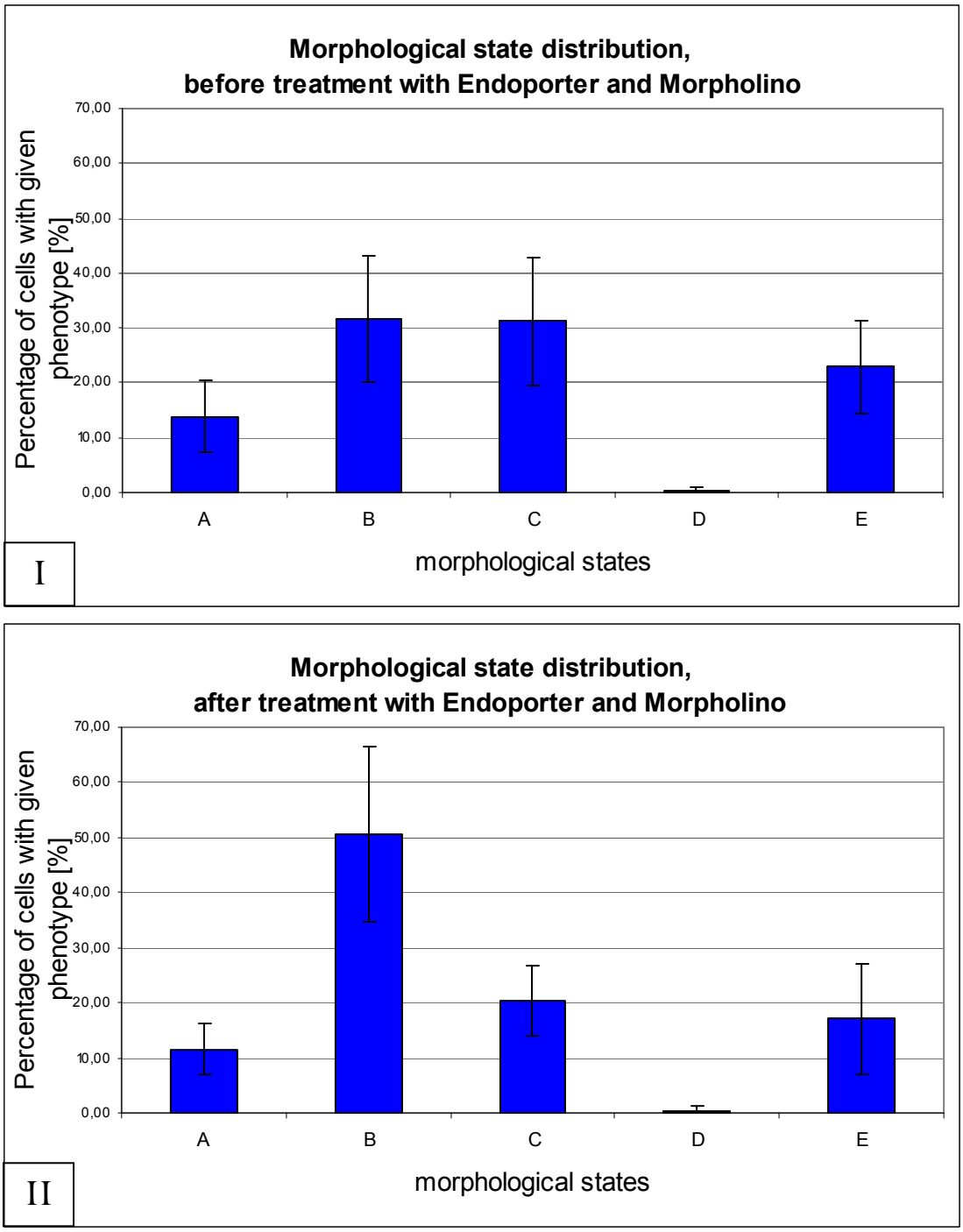

Figure 32. Cell state distribution before and 24 hours after treatment with Endoporter; combined data from two representative studies. Please note that the percentages of cell phenotypes (I) before treatment differ to Figure 30 (I), since these experiments were done separately. (A: dead, B: amoeboid, C: bipolar, D: long-processed, E: multipolar)

Again, giving a better overview of these two charts, the proportional change of each morphological state due to Endoporter treatment is shown underneath (Figure 33).

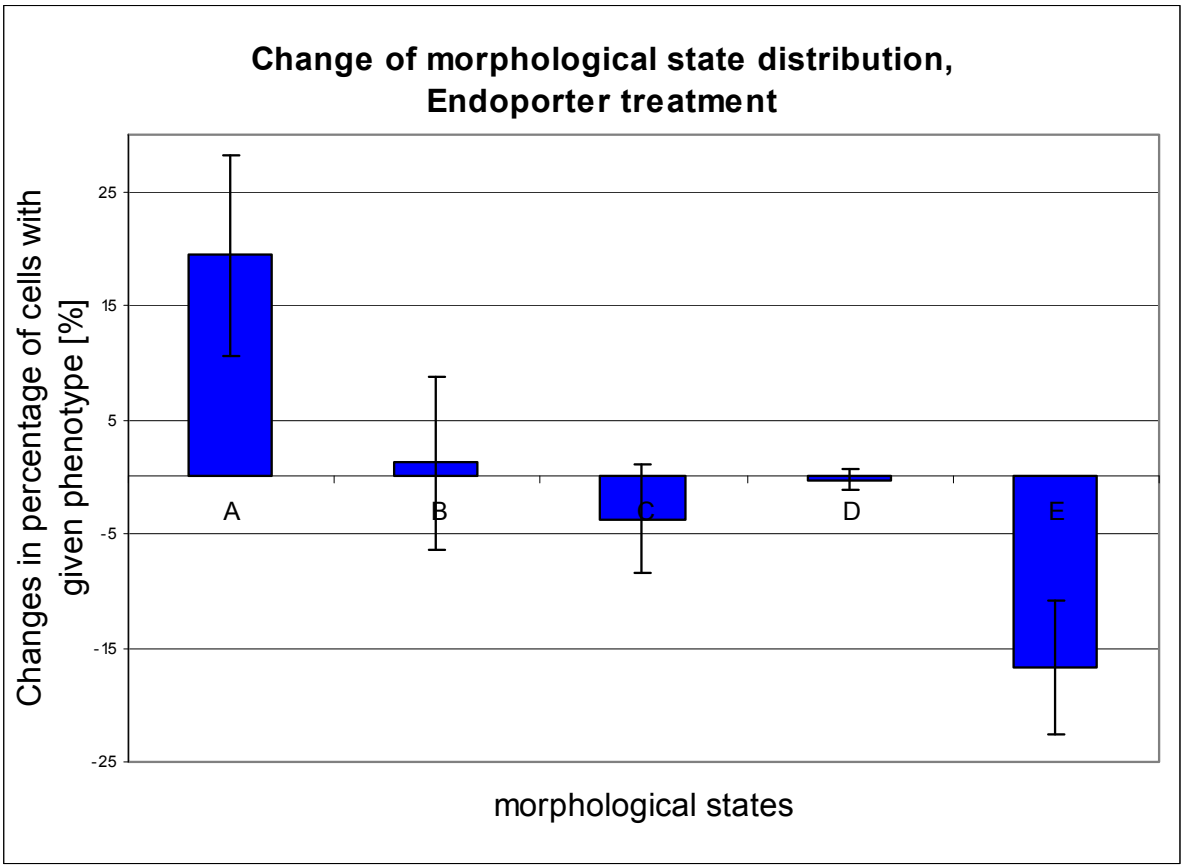

Figure 33. Change of morphological cell state distribution from before treatment to 24 hours after treatment with Endoporter; combined data from two representative studies. (A: dead, B: amoeboid, C: bipolar, D: long-processed, E: multipolar)

These data clearly indicated that treatment with Endoporter only did not lead to an increase in the number of amoeboid MG.

We wanted to compare the treatment with Endoporter only to the treatment with Endoporter plus Dscam Morpholino. For this purpose, we first determined the average percentage of untreated cells with a given phenotype from four different experimental setups (Figure 34).

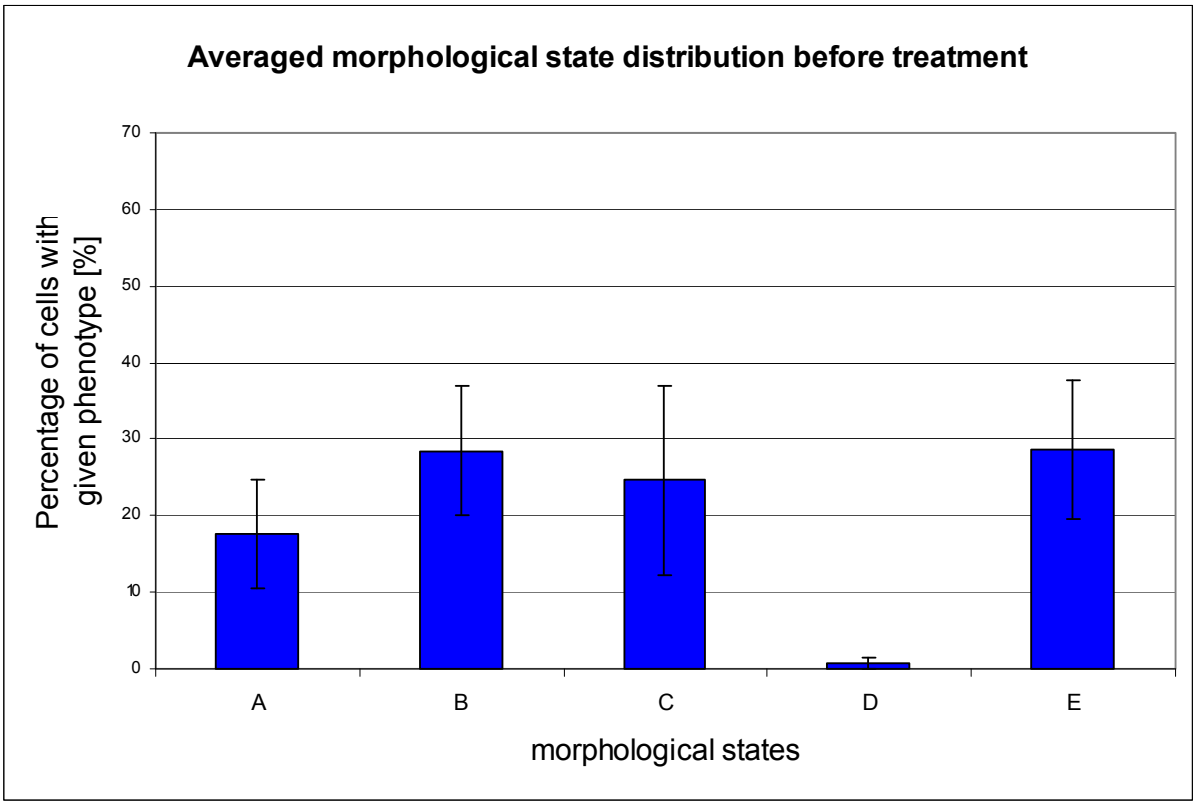

Figure 34. Averaged numbers of cells with a given phenotype, obtained from four different experimental setups. (A: dead, B: amoeboid, C: bipolar, D: long-processed, E: multipolar)

I next subtracted the percentages before treatment from the percentages of the endoporter treated cells (Δ_1) or from the Endoporter plus Morpholino treated cells (Δ_2). To clearly reveal the effects of the Dscam Morpholinos, I then subtracted Δ_1 from Δ_2 (Table 9, Figure 35).

	A	B	C	D	E
before treatment	17,56	28,51	24,62	0,64	28,67
Endoporter only	39,56	27,48	16,26	0,63	16,08
Δ_1	22,00	-1,03	-8,36	-0,01	-12,59
before treatment	17,56	28,51	24,62	0,64	28,67
Endoporter plus Morpholino	11,53	50,59	20,36	0,37	17,15
Δ_2	-6,03	22,08	-4,26	-0,27	-11,52
Δ_2-Δ_1	**-28,03**	**23,11**	**4,10**	**-0,26**	**1,08**

Table 9. Percentages of cells with given phenotypes before treatment (averaged) and after treatment with Endoporter and with Endoporter plus Dscam Morpholino. Changes ($\Delta_{1/2}$) in percentages of cells with given phenotype for Endoporter and Endoporter plus Dscam Morpholino treatment, relating to averaged percentages before treatment. The final result, the effect caused by Dscam Morpholino is given by Δ_2-Δ_1. (Phenotypes: dead (A), amoeboid (B), bipolar (C), long-processed (D) and multipolar (E))

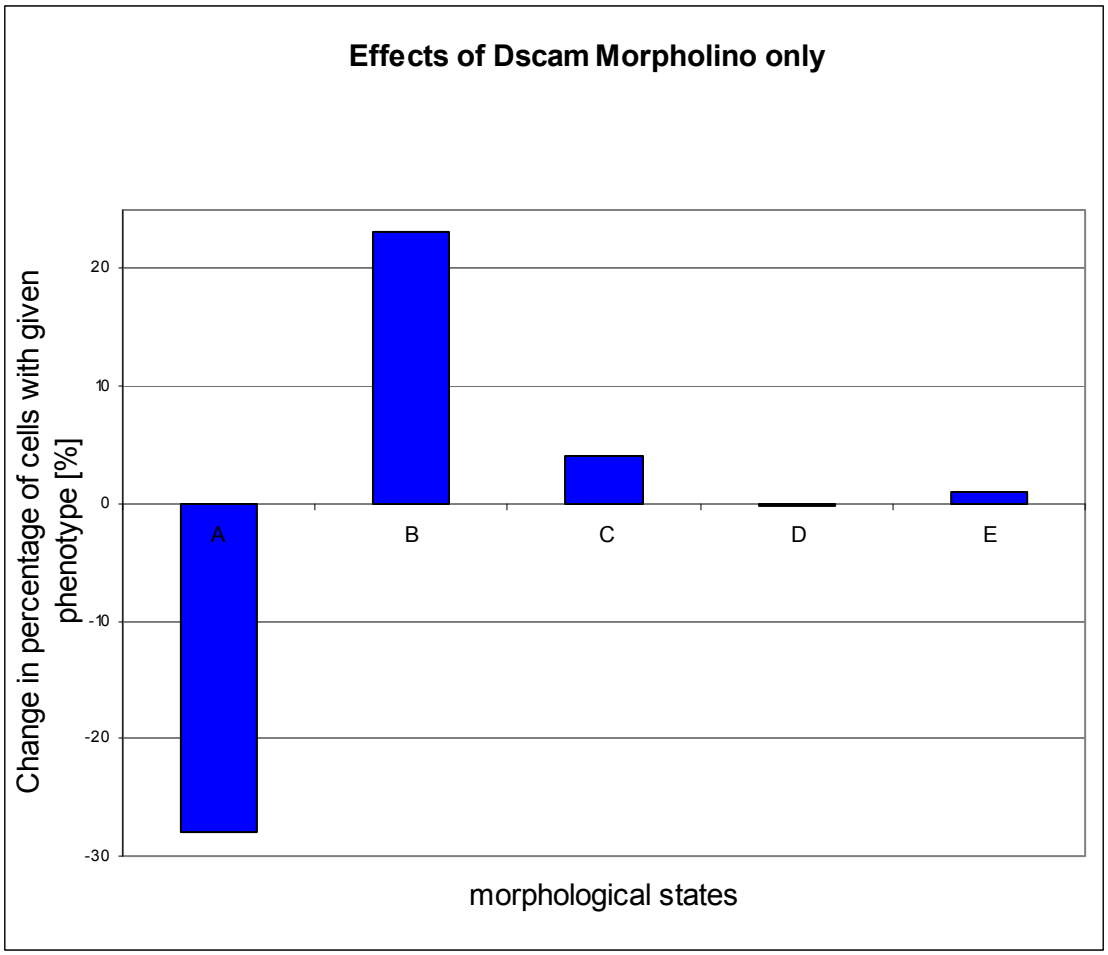

Figure 35. Effects of Dscam Morpholino only. Change in percentages of cells with given phenotype from before treatment to 24 hours after treatment with Dscam Morpholino, calculated by subtraction of sole Endoporter effect from Endoporter/Morpholino treatment; combined data from two Endoporter plus Morpholino and two Endoporter studies, relating to averaged cell percentages before treatment of all four studies. (A: dead, B: amoeboid, C: bipolar, D: long-processed, E: multipolar)

Dscam morpholinos seem to strongly enhance the formation of an amoeboid (B), and to a much lesser extent, also the bipolar (C) and multipolar (E) phenotype of MG. It is also important to note that Dscam Morpholinos seem to reduce the numbers of dead cells (A).

3. Discussion

Two different microglia populations were described in the rat, based on the expression of an antibody-reactive keratan sulfate proteoglycan (KSPG) on their cell surface (Jones and Tuszynski, 2002). Its expression rate on MG was quantified in FACS analyses and sorting, using the 5D4 monoclonal anti-KSPG antibody. Microarray studies with 5D4 sorted MG, resulted in many molecules whose expression rate is upregulated in $5D4^{high}$ MG, related to their $5D4^{low}$ counterpart (Leitner and Bradl, unpublished observation). We chose five of these molecules which were of particular interest, concerning MG development and function: Cadm1, Dlx2, Dscam, Tef, and Twist-2.

At the beginning of my work, we wanted to confirm if all of them were really expressed in MG. PCR analysis revealed that four of these five genes were expressed in MG from the 2^{nd} shake off: Dlx2, Dscam, Tef, and Twist-2.

Down syndrome cell adhesion molecule (Dscam) is known as phagocytic receptor and as an opsonin in Drosophila. Thus, it was the most interesting gene for us.

Dscam was initially found to be involved in neural development (Yamakawa et al., 1998). The Drosophila Dscam gene consists of twenty-four exons, four of them undergoing mutually exclusive alternative splicing, generating a potential of 38,016 receptor isoforms (Crayton et al., 2006). They are expressed in the nervous and immune system of flies and it has been shown that these molecules are functionally required in both systems (Chen et al., 2006). Crystallographic analyses revealed a horseshoe-shaped configuration of the Dscam protein (see 1.Introduction, Meijers et al., 2007) and either side of the molecule presents a distinct surface epitope generated by its hypervariable amino acid residues. Epitope I allows to form a homodimer for intrinsic self-recognition, whereas epitope II contributes to heterophilic binding, such as netrin or pathogenic molecules (Stuart and Ezekowitz, 2008). An unprecendented expansion of complex alternative splicing has been uniquely employed by arthropods to generate diverse surface receptors, important for cell-cell communication, molecular self recognition in neurons, and innate defenses (Figure 36, Schmucker and Chen, 2009).

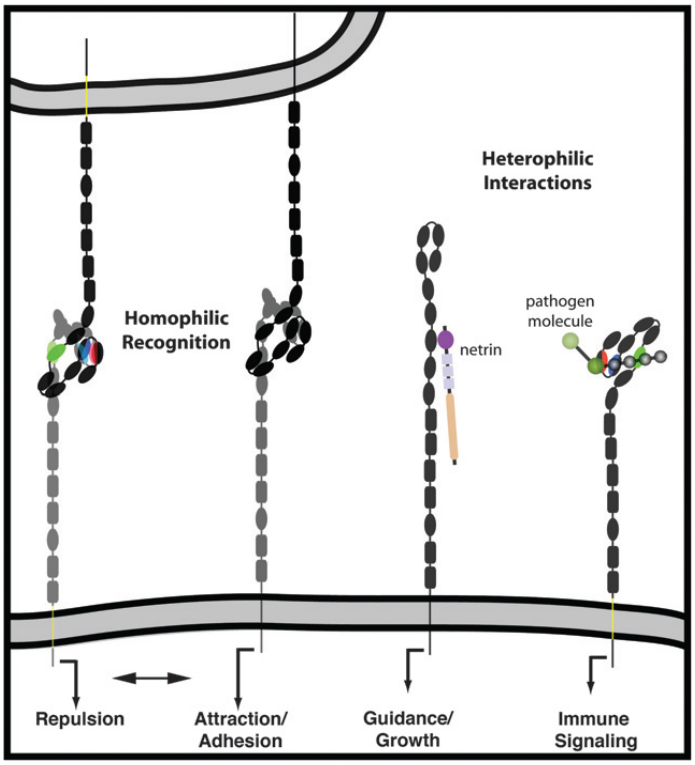

Figure 36. Dscam homophilic and heterophilic interactions for signalling, inducing multiple functions (Figure taken from Schmucker and Chen, 2009)

Homophilic interactions do not simply result in adhesion but rather constitute a recognition event that triggers diverse cellular responses, crucial for neural wiring. Sister-dendrites, expressing the same Dscam isoform, prevent from self crossing by Dscam-dependent repulsion. Dendrites of neighbouring neurons seem to use a Dscam- independent process for repulsion (Figure 37, Schmucker, 2007).

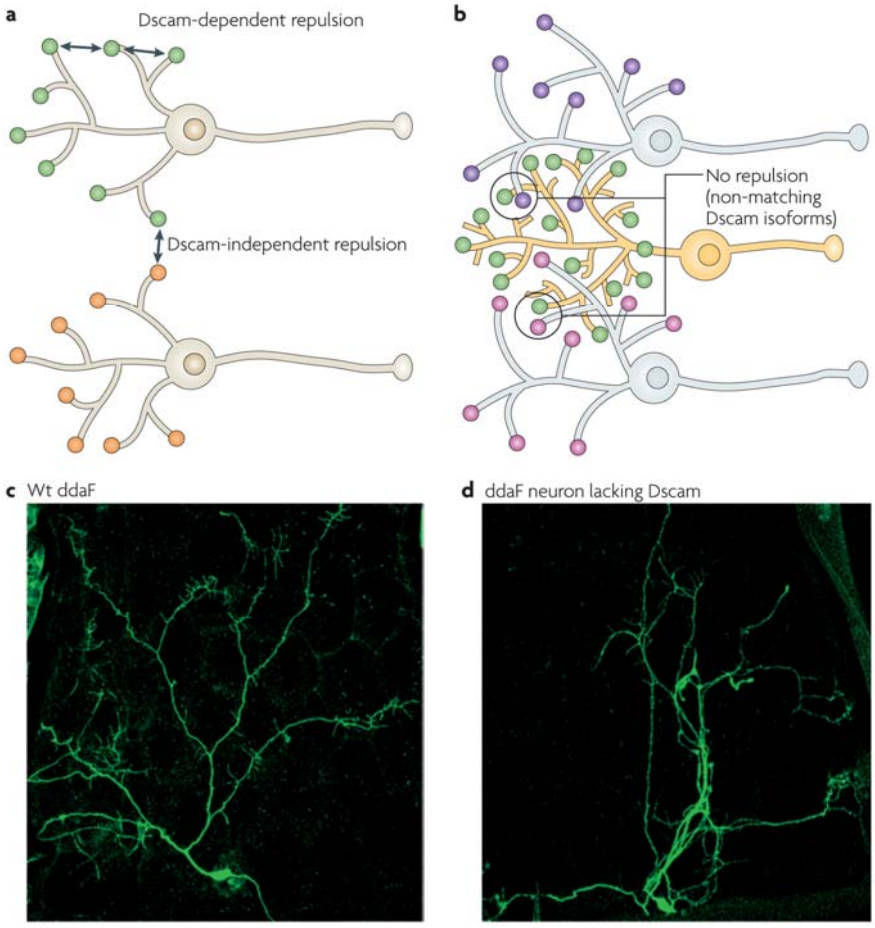

Figure 37. Homophilic recognition of identical Dscam isoforms mediates repulsion and dendrite self-avoidance. a | Dscam is specifically required for cell-intrinsic recognition. Sister dendrites expressing the same isoform are repelled by Dscam-dependent signalling, thereby preventing selfcrossing. However, the dendrite–dendrite repulsion of neighbouring neurons (that is, dendrite tiling) does not require Dscam function. b | To allow the overlap of dendritic fields (tolerance), Dscam repulsion must be blocked. This is achieved by the fact that different neurons express different isoforms, which fail to interact homophilically and therefore fail to trigger repulsion. c | Multidendritic neurons develop highly branched dendritic branches, but none of the branches exhibit self-crossing. A wildtype (Wt) example of a Drosophila melanogaster class III peripheral neuron (ddaF) is shown. d | Loss of Dscam in a ddaF neuron abolishes self-avoidance, resulting in excessive self-crossing and even abnormal fasciculation of dendritic branches (Figure and legend taken from Schmucker, 2007).

In Drosophila, a potential for more than 18,000 isoforms of Dscam on immune-competent cells was found. Additionally, a secreted protein isoform was detected in the hemolymph, and its loss derogates the efficiency of phagocytosis (Watson et al., 2005). Apparently, many functional characteristics are shared by antibodies in mammals and Dscam in Drosophila. Both, Dscam on Drosophila haemocytes und B cell receptors (BCRs) on mammalian B cells, recognize foreign antigen and transmit signals, leading to cell activation or survival. This induces production of opsonin-acting secreted forms of both, Dscam or immunoglobulin respectively. In mammals immunoglobulin is bound by Fc receptors, but in Drosophila haematocytes it is unclear wether Dscam-opsonized particles are bound by a dedicated

receptor or through homotypic interactions with membrane-bound Dscam. Both, BCR and Dscam, can also act as endocytic or phagocytic surface receptors to internalize antigens or pathogens (Figure 38, Stuart and Ezekowitz, 2008).

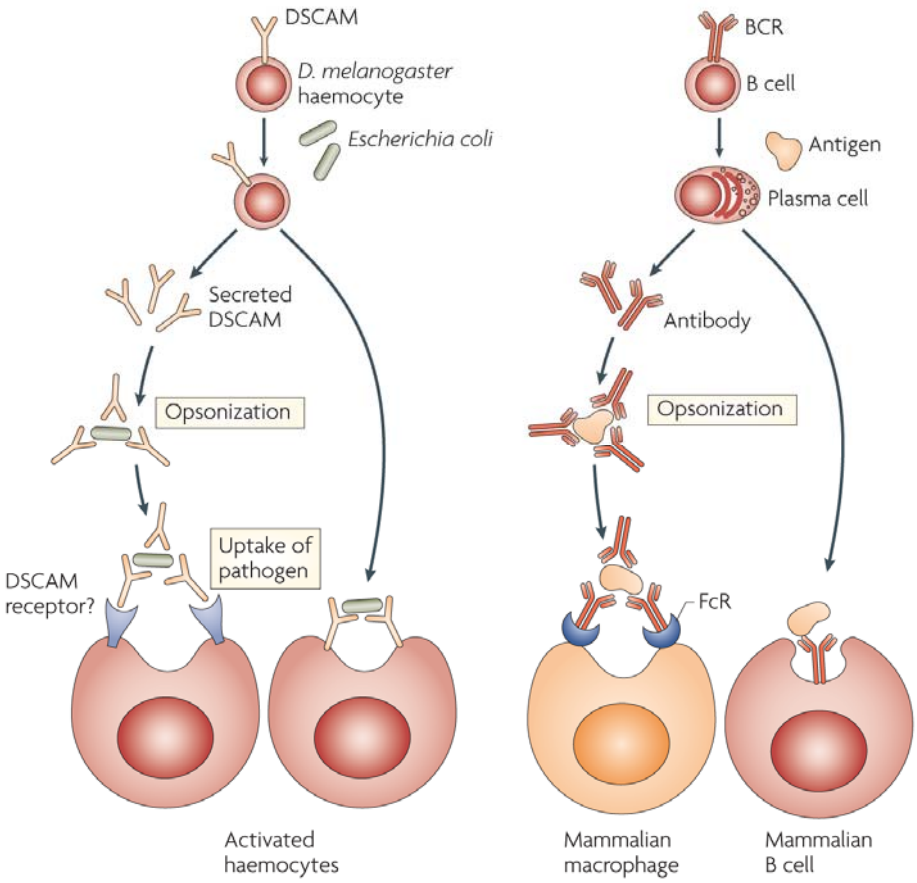

Figure 38. Insect Dscam and mammalian immunoglobulins show common functional characteristics: recognition/binding of foreign antigen, followed by activation of cells (or survival) and production of opsonin-acting secreted molecules; additionally, both can also act as cell surface bound phagocytic/endocytic receptor; (Figure taken from Stuart and Ezekowitz, 2008).

It might be possible that Dscam, similar to many chemokines has both, a neuronal and a immunological relevance in mammals. Chemokines, which regulate diverse functions in the immune system, were initially thought to play a role in leukocyte migration and neuroinflammation. Later, they were found to be expressed by all major cell types in the CNS. Interestingly, CCR2, a chemokine receptor that binds to both CCL2 and CCL7, is expressed by neurons and glia in the adult rat brain (Edman et al., 2008). Another chemokine, 58 CXCL12 was initially reported as a bone marrow stromal cell-derived chemoattractant and proliferative factor for B cell precursors. More recently, studies have demonstrated the roles

of CXCL12, and its receptor, CXCR4, in multiple aspects of B and T cell development and in effector immune responses. CXCL12 was found to be constitutively expressed by a variety of parenchymal tissues, including the CNS where it participates in neuronal proliferation, migration, axonal pathfinding, and myelination during development.

PCR analysis with Dscam_middle, representing the C-terminal, intracellular part of the Dscam protein, showed the presence of its mRNA in microglia from the 2nd shake off and in sorted microglia (CD45^{low}) from healthy and PLP transgenic rat spinal cords, whereas macrophages from peritoneum and sorted macrophages (CD45^{high}) from spinal cord and spleen appeared to be Dscam negative. Products from the N- termius of Dscam, using the Dscam_large primers, were also obtained from microglia from the 2nd shake off.

Further, we wanted to investigate the protein level of Dscam. We did a Western blot analysis and expected a band in the range of 222,3 kDa (reported sequence in the NCBI database (National Center of Biotechnology Information)). Both trials yielded an unexpected band at ~ 100 kDa for both, protein from rat microglia from the 2nd shake off and from rat brain (as control) (see 2.2.). Immuncytochemical stainings resulted in Dscam positive cells, but since these results were not convincing enough, we wanted to confirm our findings with FACS analysis. Unfortunately, we were not able to obtain clean Dscam positive and negative populations with our Dscam antibody in FACS analysis (2.4.1).

A possible reason for our findings could be that our available antibody, goat anti-human Dscam, was not suitable for our purposes. An unknown splice variant could explain the smallish band we had observed. But it is more likely that the antibody bound to another rat protein which had a high sequence homology to human Dscam.

Otherwise, low signals, received in Western blot analysis and immuncytochemical stainings, maybe showed up owing to an impurity of our samples due to neuronal contaminants. FACS sorts with just 1-2% impurity of non-target cells, which highly express Dscam, may lead to signals in microarray studies and even in PCR.

Finally, we performed a functional knock down experiment in cultured MG, based on an Endoporter mediated endocytosis of Dscam Morpholinos. Unfortunately, we were not able to prove that we achieved a successful knock down with our protein analysis methods. Nevertheless, we revealed an interesting effect of the Dscam Morpholino treatment: The formation of amoeboid MG seemed to be strongly enhanced. MG of this phenotype are

known to be activated phagocytes (Ling, 1976). Nonoverlapping coverage of receptive territories is ensured by cell-specific repulsive interactions in the development of neuron arbors and there is strong evidence that Dscam mediates this contact-dependent process (Matthews et al., 2007). Based on this knowledge and assumed that Dscam is expressed in MG, one would suppose that MG would loose their ability to cover non-overlapping territories due to Dscam knock down. Hence, we speculate that Dscam could mediate this MG- typic process to cover non-overlapping territories. As this is the case, knock down of this gene could lead to a loss of their ability to form processes and they would develop the phagocytic phenotype.

Future experiments should be done to gain more information about the role of Dscam in mammals. A rat specific anti-Dscam antibody would help to propose clear statements about Dscam expression in rat MG. Additionally, novel fundamental knowledge about the diversity of MG populations could lead to new therapeutic approaches.

4. References

Aboul-Enein, F., Bauer, J., Klein, M., Schubart, A., Flugel, A., Ritter, T., Kawakami, N., Siedler, F., Linington, C., Wekerle, H., *et al.* (2004). Selective and antigen-dependent effects of myelin degeneration on central nervous system inflammation. J Neuropathol Exp Neurol *63*, 1284-1296.

Alliot, F., Godin, I., and Pessac, B. (1999). Microglia derive from progenitors, originating from the yolk sac, and which proliferate in the brain. Brain Res Dev Brain Res *117*, 145-152.

Chen, B.E., Kondo, M., Garnier, A., Watson, F.L., Puettmann-Holgado, R., Lamar, D.R., and Schmucker, D. (2006). The molecular diversity of Dscam is functionally required for neuronal wiring specificity in Drosophila. Cell *125*, 607-620.

Crayton, M.E., 3rd, Powell, B.C., Vision, T.J., and Giddings, M.C. (2006). Tracking the evolution of alternatively spliced exons within the Dscam family. BMC Evol Biol *6*, 16.

Del Rio-Hortega, P. (1932). Microglia. In Cytology & Cellular Pathology of the Nervous System. W Penfield, ed (New York, Hafner), pp. 482–534.

Dodt, H.U., Leischner, U., Schierloh, A., Jahrling, N., Mauch, C.P., Deininger, K., Deussing, J.M., Eder, M., Zieglgansberger, W., and Becker, K. (2007). Ultramicroscopy: three-dimensional visualization of neuronal networks in the whole mouse brain. Nat Methods *4*, 331-336.

Edman, L.C., Mira, H., and Arenas, E. (2008). The beta-chemokines CCL2 and CCL7 are two novel differentiation factors for midbrain dopaminergic precursors and neurons. Exp Cell Res *314*, 2123-2130.

Fuerst, P.G., Koizumi, A., Masland, R.H., and Burgess, R.W. (2008). Neurite arborization and mosaic spacing in the mouse retina require DSCAM. Nature *451*, 470-474.

Galibert, L., Diemer, G.S., Liu, Z., Johnson, R.S., Smith, J.L., Walzer, T., Comeau, M.R., Rauch, C.T., Wolfson, M.F., Sorensen, R.A., *et al.* (2005). Nectin-like protein 2 defines a subset of T-cell zone dendritic cells and is a ligand for class-I-restricted T-cell-associated molecule. J Biol Chem *280*, 21955-21964.

Inukai, T., Inaba, T., Dang, J., Kuribara, R., Ozawa, K., Miyajima, A., Wu, W., Look, A.T., Arinobu, Y., Iwasaki, H., *et al.* (2005). TEF, an antiapoptotic bZIP transcription factor related to the oncogenic E2A-HLF chimera, inhibits cell growth by down-regulating expression of the common beta chain of cytokine receptors. Blood *105*, 4437-4444.

Jander, S., Schroeter, M., Fischer, J., and Stoll, G. (2000). Differential regulation of microglial keratan sulfate immunoreactivity by proinflammatory cytokines and colony-stimulating factors. Glia *30*, 401-410.

Jander, S., and Stoll, G. (1996). Strain-specific expression of microglial keratan sulfate proteoglycans in the normal rat central nervous system: inverse correlation with constitutive expression of major histocompatibility complex class II antigens. Glia *18*, 255-260.

Jones, L.L., and Tuszynski, M.H. (2002). Spinal cord injury elicits expression of keratan sulfate proteoglycans by macrophages, reactive microglia, and oligodendrocyte progenitors. J Neurosci *22*, 4611-4624.

Kreutzberg, G.W. (1995). Microglia, the first line of defence in brain pathologies. Arzneimittelforschung *45*, 357-360.

Kreutzberg, G.W. (1996). Microglia: a sensor for pathological events in the CNS. Trends Neurosci *19*, 312-318.

Ling, E.A. (1976). Some aspects of amoeboid microglia in the corpus callosum and neighbouring regions of neonatal rats. J Anat *121*, 29-45.

Matthews, B.J., Kim, M.E., Flanagan, J.J., Hattori, D., Clemens, J.C., Zipursky, S.L., and Grueber, W.B. (2007). Dendrite self-avoidance is controlled by Dscam. Cell *129*, 593-604.

Meijers, R., Puettmann-Holgado, R., Skiniotis, G., Liu, J.H., Walz, T., Wang, J.H., and Schmucker, D. (2007). Structural basis of Dscam isoform specificity. Nature *449*, 487-491.

Paxinos, G., and Watson, C. (2007). The rat brain in stereotaxic coordinates. Academic Press.

Raivich, G. (2005). Like cops on the beat: the active role of resting microglia. Trends Neurosci *28*, 571-573.

Ritter, M.R., Banin, E., Moreno, S.K., Aguilar, E., Dorrell, M.I., and Friedlander, M. (2006). Myeloid progenitors differentiate into microglia and promote vascular repair in a model of ischemic retinopathy. J Clin Invest *116*, 3266-3276.

Rozen, S., and Skaletsky, H. (2000). Primer3 on the WWW for general users and for biologist programmers. Methods Mol Biol *132*, 365-386.

Schmid, C.D., Sautkulis, L.N., Danielson, P.E., Cooper, J., Hasel, K.W., Hilbush, B.S., Sutcliffe, J.G., and Carson, M.J. (2002). Heterogeneous expression of the triggering receptor expressed on myeloid cells-2 on adult murine microglia. J Neurochem *83*, 1309-1320.

Schmucker, D. (2007). Molecular diversity of Dscam: recognition of molecular identity in neuronal wiring. Nat Rev Neurosci *8*, 915-920.

Schmucker, D., and Chen, B. (2009). Dscam and DSCAM: complex genes in simple animals, complex animals yet simple genes. Genes Dev *23*, 147-156.

Sharabi, A.B., Aldrich, M., Sosic, D., Olson, E.N., Friedman, A.D., Lee, S.H., and Chen, S.Y. (2008). Twist-2 controls myeloid lineage development and function. PLoS Biol *6*, e316.

Stuart, L.M., and Ezekowitz, R.A. (2008). Phagocytosis and comparative innate immunity: learning on the fly. Nat Rev Immunol *8*, 131-141.

Sunwoo, J.B., Kim, S., Yang, L., Naik, T., Higuchi, D.A., Rubenstein, J.L., and Yokoyama, W.M. (2008). Distal-less homeobox transcription factors regulate development and maturation of natural killer cells. Proc Natl Acad Sci U S A *105*, 10877-10882.

Takahashi, K., Rochford, C.D., and Neumann, H. (2005). Clearance of apoptotic neurons without inflammation by microglial triggering receptor expressed on myeloid cells-2. J Exp Med *201*, 647-657.

Watson, F.L., Puttmann-Holgado, R., Thomas, F., Lamar, D.L., Hughes, M., Kondo, M., Rebel, V.I., and Schmucker, D. (2005). Extensive diversity of Ig-superfamily proteins in the immune system of insects. Science *309*, 1874-1878.

Yamakawa, K., Huot, Y.K., Haendelt, M.A., Hubert, R., Chen, X.N., Lyons, G.E., and Korenberg, J.R. (1998). DSCAM: a novel member of the immunoglobulin superfamily maps in a Down syndrome region and is involved in the development of the nervous system. Hum Mol Genet *7*, 227-237.

Zhang, C., Lam, T.T., and Tso, M.O. (2005). Heterogeneous populations of microglia/macrophages in the retina and their activation after retinal ischemia and reperfusion injury. Exp Eye Res *81*, 700-709.

Acknowledgements

First of all, I would like to express my sincere gratitude to Dr. Monika Bradl for giving me the opportunity to do my diploma thesis in her group. I want to thank her for her patient and excellent support, which made this project to a great experience for me.

Additionally, I would like to thank…

- my colleagues, Eva, Mesi, Rakhi, Rui, Milena and Maria, for their great cooperation and fun times besides work.
- Dieter Prinz from the St. Anna Kinderspital, for his great work in analysing and sorting many samples for me.
- Peter, who did an internship in our group, for his effort and good teamwork.
- all other people from of the centre of brain research. It was fantastic to work in this pleasant and multifarious environment.

Finally, I want to thank the most important people of my life, my family, my girlfriend Conny and all my friends, who are always there for me. Especially, I want to thank my parents for their mental and financial support not only during my studies but also in my whole life.

Curriculum Vitae

Prielhofer Roland

Personal Data:

ADDRESS	**Floßgasse 9/15, 1020 Wien, Austria**
DATE OF BIRTH	**4.4.1984**
PLACE OF BIRTH	**Wels, Austria**
MOBILE NUMBER	**(+43) 0680/1107648**
E-MAIL	**prielhofer_roland@gmx.at**

Education:

02/2009 – 08/2009	**Diploma thesis in the group of Univ.-Doz. Dr. Monika Bradl** **Center for Brain Research** **Division: Neuroimmunology** **Head: Univ.-Prof. Dr. Hans Lassmann** **Medical University of Vienna, Austria**
2004 – 2009	**Studies of Molecular Biology** **Emphases: Bioinformatics, Immunology and Neuroscience** **University of Vienna, Austria**
1998 – 2003	**Higher technical school (HTL) for chemical engineering in Wels, Austria**
1990 – 1998	**Compulsory education**